Attn: A. L. Jarrett

LWP - 1083
Copy No. 14

LANGLEY WORKING PAPER

INVESTIGATION OF THE STATIC LIFT CAPABILITY OF A LOW-ASPECT-RATIO WING OPERATING IN A POWERED GROUND-EFFECT MODE

By Jarrett K. Huffman and Charlie M. Jackson, Jr.

Langley Research Center
Hampton, Va.

This paper is given limited distribution and is subject to possible incorporation in a formal NASA report.

NATIONAL AERONAUTICS AND SPACE ADMINISTRATION

December 1, 1972

LWP - 1083

December 1, 1972

LANGLEY WORKING PAPER

INVESTIGATION OF THE STATIC LIFT CAPABILITY OF A LOW-ASPECT-RATIO WING OPERATING IN A POWERED GROUND-EFFECT MODE

Prepared by

Jarrett K. Huffman

Charlie M. Jackson, Jr.

Approved by Mark R. Nichols
Mark R. Nichols
Chief, High-Speed Aircraft Division

Approved for distribution by R. E. Bower
Robert E. Bower
Director for Aeronautics

LANGLEY RESEARCH CENTER

NATIONAL AERONAUTICS AND SPACE ADMINISTRATION

NATIONAL AERONAUTICS AND SPACE ADMINISTRATION

Langley Working Paper No. 1083

INVESTIGATION OF THE STATIC LIFT CAPABILITY OF A LOW-ASPECT-RATIO WING OPERATING IN A POWERED GROUND-EFFECT MODE

By Jarrett K. Huffman and Charlie M. Jackson, Jr.

SUMMARY

A preliminary experimental investigation has been made to evaluate the powered ground-effect capability of a low-aspect-ratio, wing-body configuration with forward-mounted propulsion. The tests were limited to static ground-effect conditions in order to obtain information on an air-cushion mode of operation. The results indicate in general that the powered ground-effect mode is within the capability of the type of configuration examined. The conditions examined indicated the possibility of hover mode and also forward acceleration capability in near-ground effect. Center-of-pressure movement did not appear to be a problem. However, it was recognized that longitudinal trim would be a problem to consider in both the hover and acceleration modes. It is felt that the results of this investigation have demonstrated sufficient potential to warrant further investigation of powered ground-effect modes of operation for low-aspect-ratio wing systems with forward-mounted propulsion.

INTRODUCTION

Over the past decade the interest in STOL and V/STOL aircraft has resulted in a considerable research effort in the area of propulsion aerodynamic integration. In order to provide good STOL performance, propulsion systems have been utilized to blow over the high-lift devices on the wing to provide lift augmentation. As a part of this research effort a somewhat unconventional method of lift augmentation has been considered for the take-off and ground handling mode of operation. The aircraft configuration considered is characterized by the location of the propulsion system in front of the wing so that the jet efflux can be directed under the wing. Unlike conventional external-blown flaps which provide lift by turning the jet efflux, the present system provides lift by producing an air cushion under a low-aspect-ratio wing. The lift is controlled at any given height by the jet efflux and a simple flap on the wing. As forward velocity increases the operating mode is similar to that of the "Ram Wing" described in reference 1. More specifically, it is an "Augmented Ram Wing" concept.

In order to obtain an insight into the potential usefulness of the "Augmented Ram Wing" concept, an experimental investigation was undertaken. The purpose of this investigation was to evaluate the static lift capability of a low-aspect-ratio wing-body configuration with forward-mounted propulsion. Existing model components were assembled to provide a low-aspect-ratio configuration with a simple flap system. The tests were limited to static conditions in order to obtain a preliminary evaluation of the capabilities of an air-cushion mode of operation. The results of these static tests are

intended to form the basis for more complex experimental investigations which will include the effects of forward velocity and transition from ground-effect to free-air mode.

SYMBOLS

The data are referred to the body-axis system with the origin of the axis located at the moment reference center shown in figure 1(a).

A	nozzle exit area, 0.970 sq in. per nozzle
c	wing chord, 12 in.
C_A	axial force coefficient, $\frac{\text{Axial force}}{(P_{T_N} - P_\infty)S}$
C_m	pitching-moment coefficient, $\frac{\text{Pitching moment}}{(P_{T_N} - P_\infty)Sc}$
C_N	normal force coefficient, $\frac{\text{Normal force}}{(P_{T_N} - P_\infty)S}$
C_p	pressure coefficient, $\frac{\text{Local groundboard pressure} - P_\infty}{(P_{T_N} - P_\infty)}$
C_μ	thrust coefficient, $\frac{2T}{(P_{T_N} - P_\infty)S}$
d	distance downstream from nozzle exit plane
h	perpendicular distance from groundboard to wing trailing edge
h_f	perpendicular distance from groundboard to flap trailing edge
P_{T_j}	total pressure in the jet
P_{T_N}	total pressure in the nozzle
P_∞	ambient pressure
S	reference area, 2.15 sq ft
T	thrust per nozzle

$\dot{W}$	nozzle weight flow
x	nozzle coordinate (see figure 1(c))
x'	longitudinal distance aft of wing leading edge
X	distance along model longitudinal axis measured positive forward from moment reference
y	nozzle coordinate (see figure 1(c))
z	nozzle coordinate (see figure 1(c))
Z	distance along model vertical axis measured positive downward from moment reference
α	groundboard angle with respect to model longitudinal axis (see figure 1(a))
δ_f	flap angle with reference to wing chord plane (see figure 1(a))
δ_j	jet deflection angle with respect to longitudinal axis (see figure 1(a))

APPARATUS AND MODEL

The present tests were conducted with a static apparatus which consisted of a model, a propulsion system, and a groundboard arranged as shown in figure 1(a). The model was sting mounted to a static stand such that the external forces and moments were measured by an internally located six-component strain-gage balance. The propulsion system which consisted of the port and starboard nozzles were mounted independent of the model so that nozzle thrust forces were not measured by the model balance. The groundboard and end plates were mounted independent of the model. In order to obtain close ground clearance data on the existing high-wing model, a hole was cut in the groundboard to provide clearance for the lower part of the fuselage. Flexible seals were used to prevent air flow between the model and groundboard at the

wing root and between the wing and end plate at the tip. Both the nozzles and groundboard were made adjustable to accommodate the variables of the test. Tests were run with the nozzle in two positions relative to the model as shown in figure 1(a). The groundboard was positioned at several heights for each of two angles (0° and 4°) during the tests. Several end plate configurations were investigated at selected nozzle and board positions. The geometric characteristics of these end plates are given in figure 1(b).

The overall characteristics of the model are given in figure 1(a). The wing has an aspect ratio of 2.15 with untapered planform and a NACA 23012 airfoil section. A full span flap was simulated by a metal bracket attached to the lower surface of the airfoil such that the effective flap chord was 0.166 c.

Figure 1(c) gives the geometric details of the nozzles. The nozzles wereinstrumented with a total head tube located just before the exit in the minimum. The contraction ratio in the nozzle was 2.06.

TESTS

Prior to the test program, a nozzle performance calibration was obtained. The nozzle control parameter was taken to be total pressure in the nozzle. The resulting nozzle thrust and weight flow variation over the total pressure range from 0 to 30 psi gage are shown in figure 2(a) for both port and starboard nozzles. The stagnation temperature of the nozzle air for this calibration and the subsequent tests was 75°F. A limited calibration of the jet decay characteristics of the port nozzle was made by surveying the maximum jet total pressure at two stations downstream of the jet exit. The results of this

survey are presented in figure 2(b) along with several comparisons of jet decay characteristics of experimental air jets from reference 2 as well as that of an actual jet engine from reference 3. These comparisons indicate the decay characteristics of the present nozzles to be relatively poor, a condition probably due to corner effects in rectangular exits.

For the entire test program, static force, moment, and groundboard surface pressure data were taken with the jets operating at a nominal jet total pressure of 12.71 psi gage. From the nozzle calibration, it can be seen that the corresponding nominal thrust and weight flow were approximately 20 pounds and 0.66 pounds per second, respectively, for each nozzle. The effects of reduced jet pressure ratio were also examined for selected test conditions.

RESULTS AND DISCUSSION

The results of the tests to determine the aerodynamic effects of jet efflux at the nominal nozzle total pressure are presented in figure 3. These results include all of the geometric parameters investigated for the basic configuration (end plate number 1). Several significant points can be obtained from the results presented in this figure. First, that the static lift of the air cushion is primarily sensitive to the clearance between the flap and groundboard (h_f/c) with the ideal maximum augmentation being when the static pressure between the undersurface of the wing and groundboard is equal to the total pressure of the jet nozzle (12.71 psi). The lift increases rapidly as the flap ground clearance nears zero with a maximum lift shown in the figure that is about 7 percent of the ideal maximum augmentation. Second, the resulting axial force is less than the axial thrust component produced by the

propulsion system ($C_\mu \cos \delta_j = 0.0109 \cos \delta_j$) which results in a net forward acceleration capability for most of the conditions of the present test. Finally, from an overall view of the results of figure 3 it can be concluded that the lift capability is considerably reduced at the very high flap angles.

The results of the zero flap tests shown in figures 3(a) and 3(b) indicate that negative lift is produced for some values of h_f/c at $\alpha = 4^\circ$ and all values of h_f/c at $\alpha = 0^\circ$. It should be noted that for the zero flap condition the minimum clearance above the groundboard occurs forward of the wing trailing edge thereby, possibly causing a venturi action of the jet flowing between the wing lower surface and the groundboard which results in the negative lift indicated in figure 3. These effects also cause the large center-of-pressure change which is reflected in the pitching-moment data of figures 3(a) and 3(b).

In addition to the force data obtained from the model balance, surface pressures were measured at three longitudinal positions (0.083 c, 0.465 c, and 0.833 c) under the wing along the jet centerline. Selected pressure distributions are presented in figure 4 corresponding to some of the test conditions of the force data of figure 3. A cursory examination of these pressure distributions verifies the behavior of the force and moment curves. For example, figure 4(b) shows the area under the zero-flap pressure distribution at $h_f/c = 0.042$ to be negative. This result agrees qualitatively with the negative normal force measured at these conditions and shown in figure 3(b). Also the high pressures shown near the wing leading edge for the zero flap condition verifies the large positive pitching moments shown in figure 3(b) for these conditions.

The effects of the end plate geometry are presented in figure 5 for the test conditions of the present investigation. In general the effects of end plates are most pronounced at the smaller values of h_f/c where the normal force is reduced as the end plate area becomes smaller. This reduction of area allows an increasing amount of jet efflux to escape at the tip of the wing thus reducing the pressure of the air cushion. As indicated by figures 5(g) and 5(h) the effects of reducing end plate area are somewhat smaller for the condition where the jet is deflected 25°. The data of figure 5 also indicates that reducing the end plate area by cutting back the leading edge did not have a significant effect on the pitch characteristics at the test conditions.

The jet total pressure was chosen to nondimensionalize the force, moment, and pressure coefficients for the present test. By virtue of this fact it is implied that proper propulsion scaling effects could be accommodated by simply applying the correct jet pressure ratio. The results of figure 6 indicate that this is not the case. The effects of reduced jet total pressure on the longitudinal aerodynamic characteristics are presented in figure 6 for several selected test conditions in the high normal force range. As is evident from the nearly constant values of their coefficients in figure 6, the pitching moment and axial force scale quite linearly with jet total pressure. Unfortunately the most important parameter, normal force, does not follow a linear relationship with jet total pressure for all of the selected conditions.

In order to summarize the potential of the concept tested, figure 7 was prepared to show the net performance of a static air-cushion mode. In figure 7, a variation of the net axial and normal forces as well as

longitudinal and vertical center of pressure is shown versus height of the wing airfoil reference line from the ground. The curves represent continuous variation of the flap to maintain constant flap trailing-edge ground clearance. It should be noted that the force coefficients and centers of pressure include the nozzle thrust effects with the nozzles operating at nominal conditions ($C_\mu = 0.0109$).

The results shown in figure 7 indicate some forward acceleration available at the high normal force conditions. For example, figure 7(a) shows that a vehicle with weight corresponding to $C_N + C_\mu \sin \delta_j = 0.07$ would possess a net axial accelerating force at $h/c = 0.078$ corresponding to $C_A - C_\mu \cos \delta_j = -0.006$ or 0.085 g's. Figure 7 also indicates the center-of-pressure movement with height to be slight for small values of flap trailing edge to ground clearance h_f/c . However, as large variations of h_f/c are considered the center-of-pressure movement can become very large.

Figure 7 can be used to evaluate the lift capability and acceleration potential of an air-cushion mode of operation. For example, consider a vehicle with wing loading, W/S , of 68 lb/ft^2 , a thrust loading, $2T/W$, of 0.274 and a chord length of 40 feet. In order to support the weight of this vehicle a net normal force coefficient of 0.04 is required. If a jet pressure ratio of 1.8 is assumed along with $\alpha = 4^\circ$ and $\delta_j = 13^\circ$ the conditions of figure 7(b) apply. If the initial condition is assumed to be $\delta_f = 16^\circ$ and wing vertical height 3.2 feet above the ground (h/c = 0.08), the vehicle would rise vertically and move forward with a 0.15 g acceleration. At a vertical height of the wing reference plane of 5.2 feet above the ground (h/c = 0.13) a

condition of vertical equilibrium would be reached with flaps at about 35° deflection, $C_N + C_\mu \sin \delta_j = 0.04$.

It should be pointed out that the previous example, and indeed this preliminary investigation, serves only to point out the potential of an air-cushion and augmented ram wing modes of operation. It is recognized that during these operations stability and trim problems result which must be solved for each specific configuration and mode considered. It is also recognized that for the augmented ram wing concept the effect of forward velocity will considerably alter the lift and moment characteristics.

The current preliminary investigation involving a configuration with a low-aspect-ratio wing and forward-mounted propulsion system has demonstrated the need to investigate in more detail a static air-cushion and augmented ram wing modes of operation.

CONCLUDING REMARKS

A preliminary experimental investigation has been made to evaluate the powered ground-effect capability of a low-aspect-ratio wing-body configuration with forward-mounted propulsion. The tests were limited to static ground-effect conditions in order to obtain information on an air-cushion mode of operation. The results indicate in general that a powered ground effect mode is within the capability of the type of configuration examined. The conditions examined indicated the possibility of hover mode and also forward acceleration capability in near-ground effect. Center-of-pressure movement did not appear to be a problem. However, it was recognized that longitudinal trim would be a problem to consider in both the hover and acceleration modes.

It is felt that the results of this investigation have demonstrated sufficient potential to warrant further investigation of powered ground-effect modes of operation for low-aspect-ratio wing systems with forward-mounted propulsion.

REFERENCES

1. Boehler, Gabriel D.: Basic Principles of Ground Cushion Devices. Preprint No. 133A, SAE, January 1960.

2. Gentry, Garl L.; and Margason, Richard J.: Jet-Induced Lift Losses on VTOL Configurations Hovering In and Out of Ground Effect. NASA TN D-3166, February 1966.

3. Margason, Richard J.; and Gentry, Garl L.: Static Calibration of an Ejector Unit for Simulation of Jet Engines In Small-Scale Wind-Tunnel Models. NASA TN D-3867, March 1967.

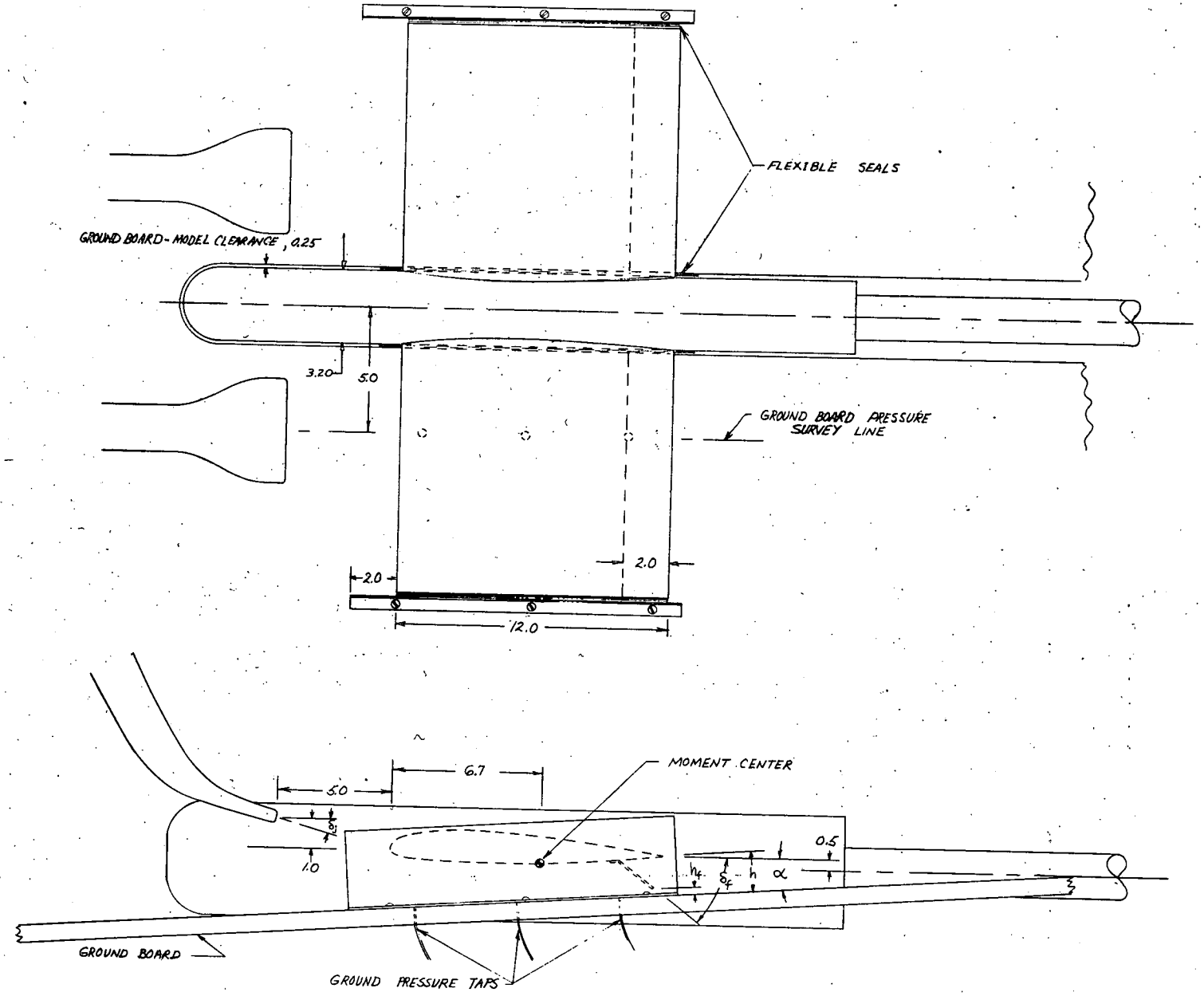

(a) Model setup with ground board.

Figure 1.- Model details (all dimensions are in inches).

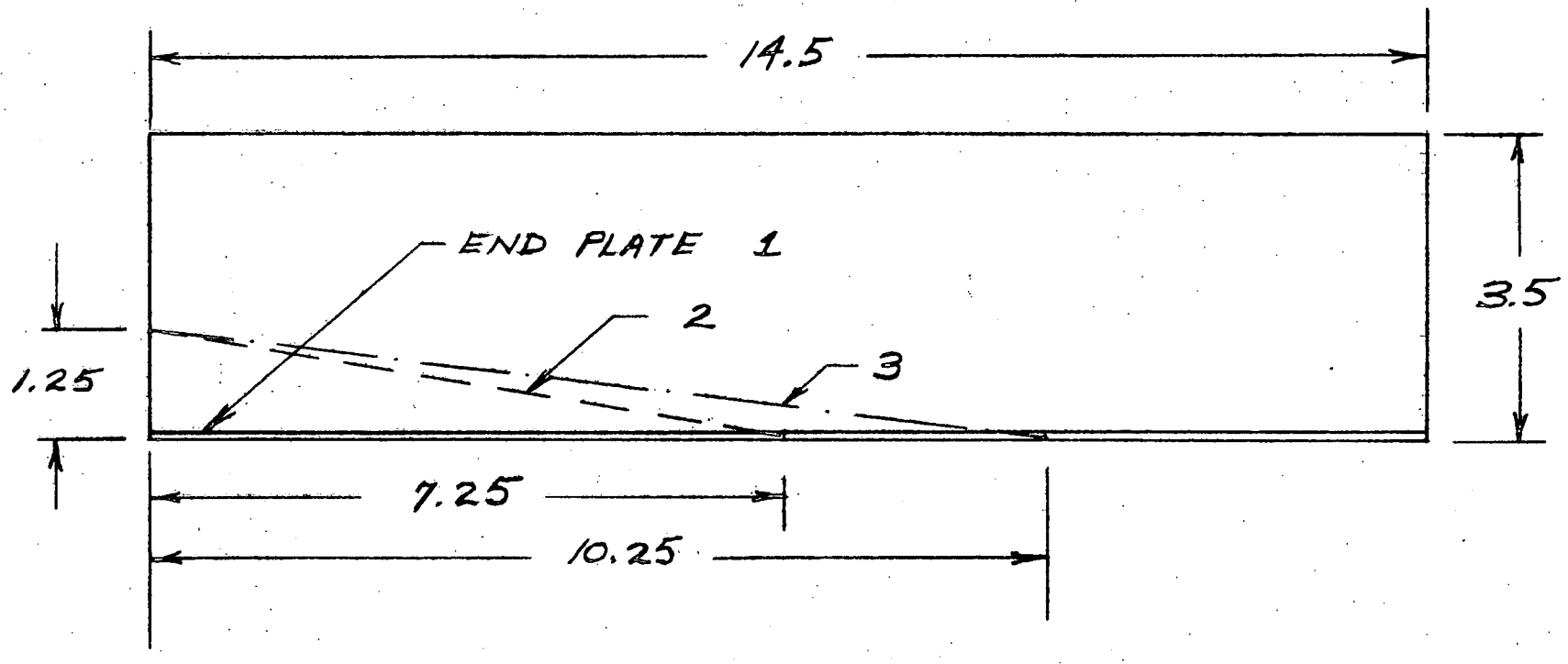

(b) End plate details.

Figure 1.- Continued.

NOZZLE INTERIOR COORDINATES

x	y	z_L	z_U
0	2.183	0	.222
1.	2.183	0	.222
2.	1.920	0	.300
3.	1.370	0	.510
4.	1.040	.040	.975
5.	.875	.290	1.700
6.	.820	.780	2.600
7.	.800	1.490	3.675
8.	.800	2.380	4.775
9.	.800	3.460	5.900

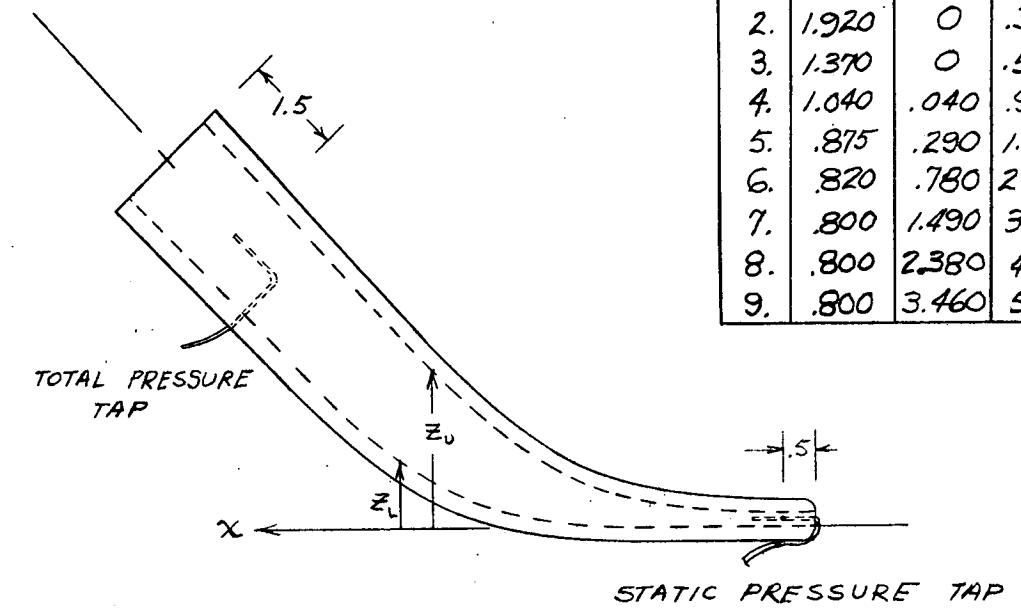

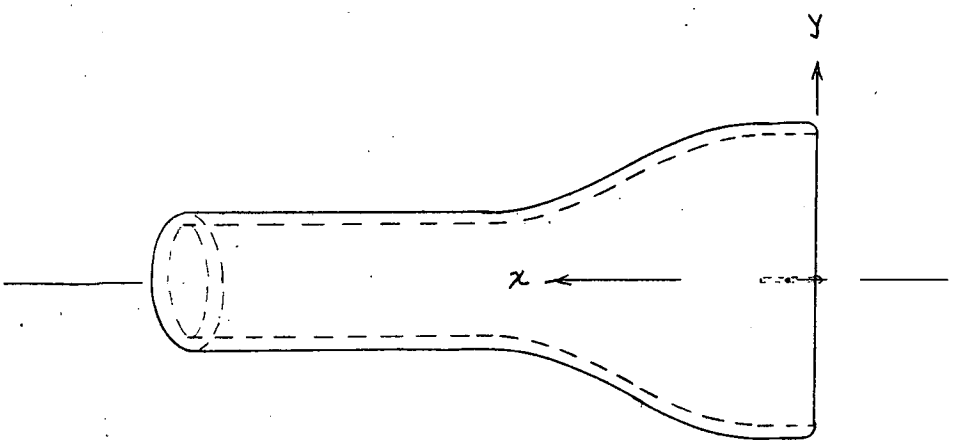

(c) Nozzle geometry.

Figure 1.- Concluded.

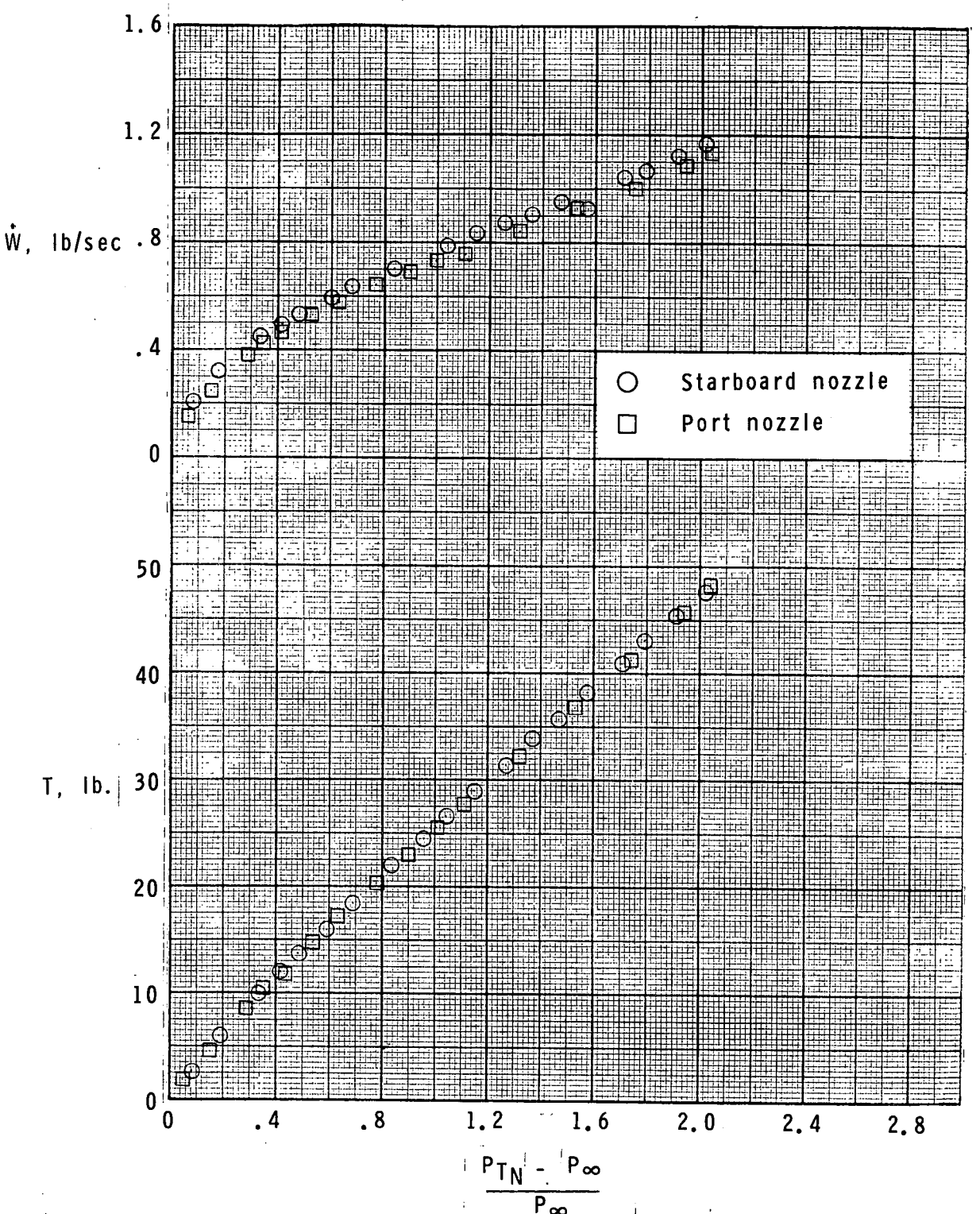

(a) Thrust and weight flow vs. total nozzle pressure.

Figure 2.- Nozzle calibrations.

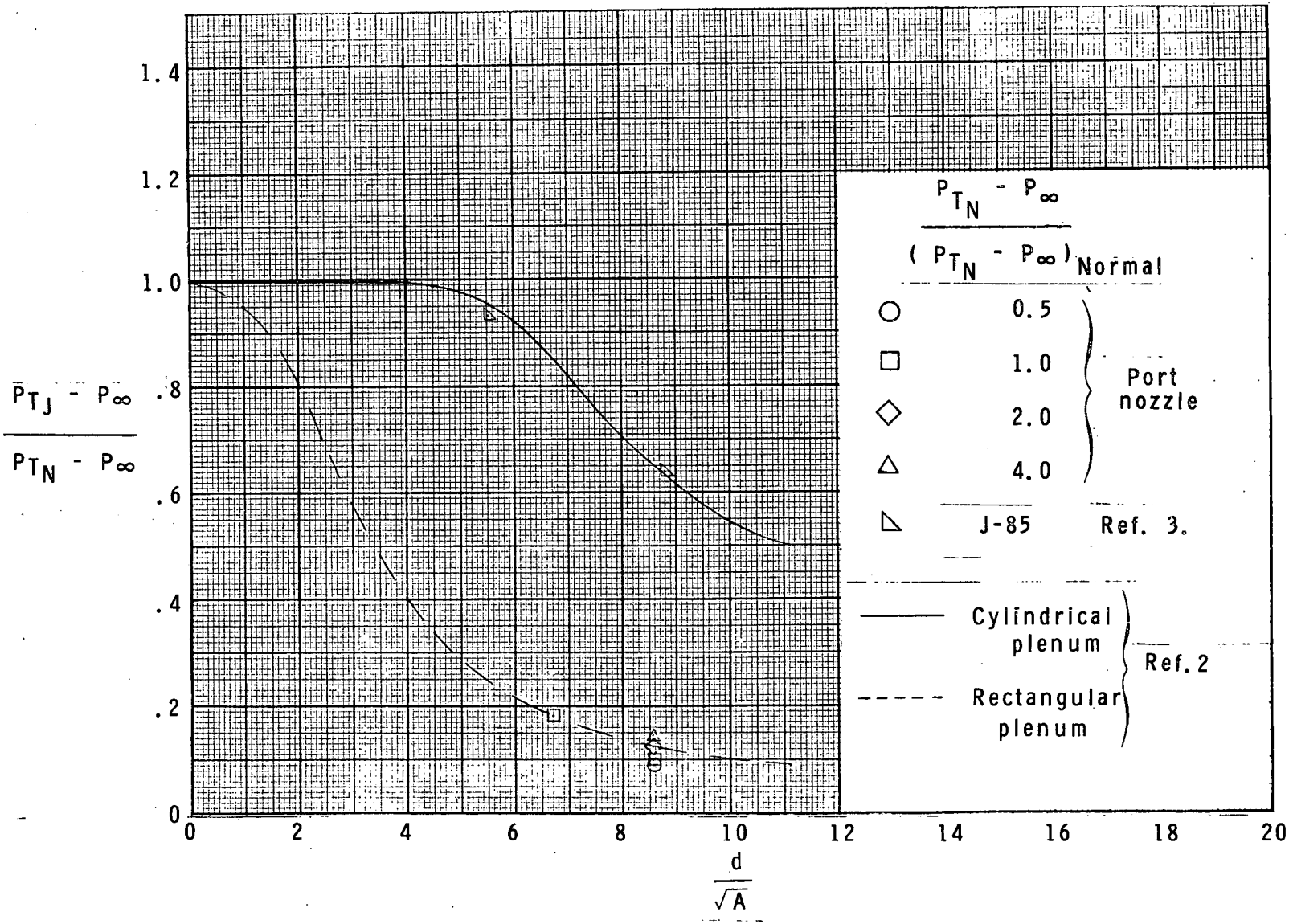

(b) Jet decay characteristics.

Figure 2.- Concluded.

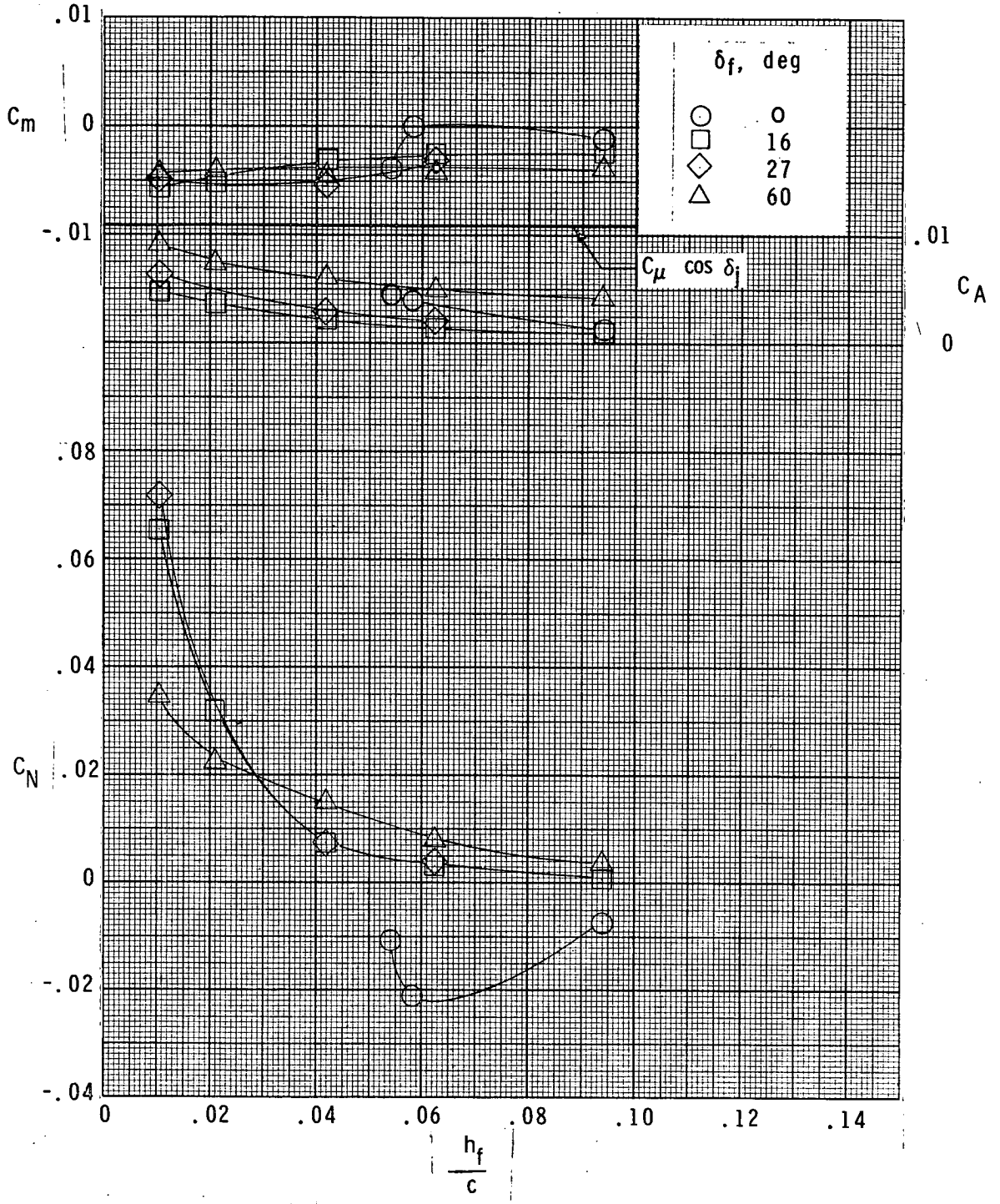

(a) $\alpha = 0°$, $\delta_j = 13°$.

Figure 3.- Jet efflux effects on longitudinal aerodynamic characteristics of basic configurati

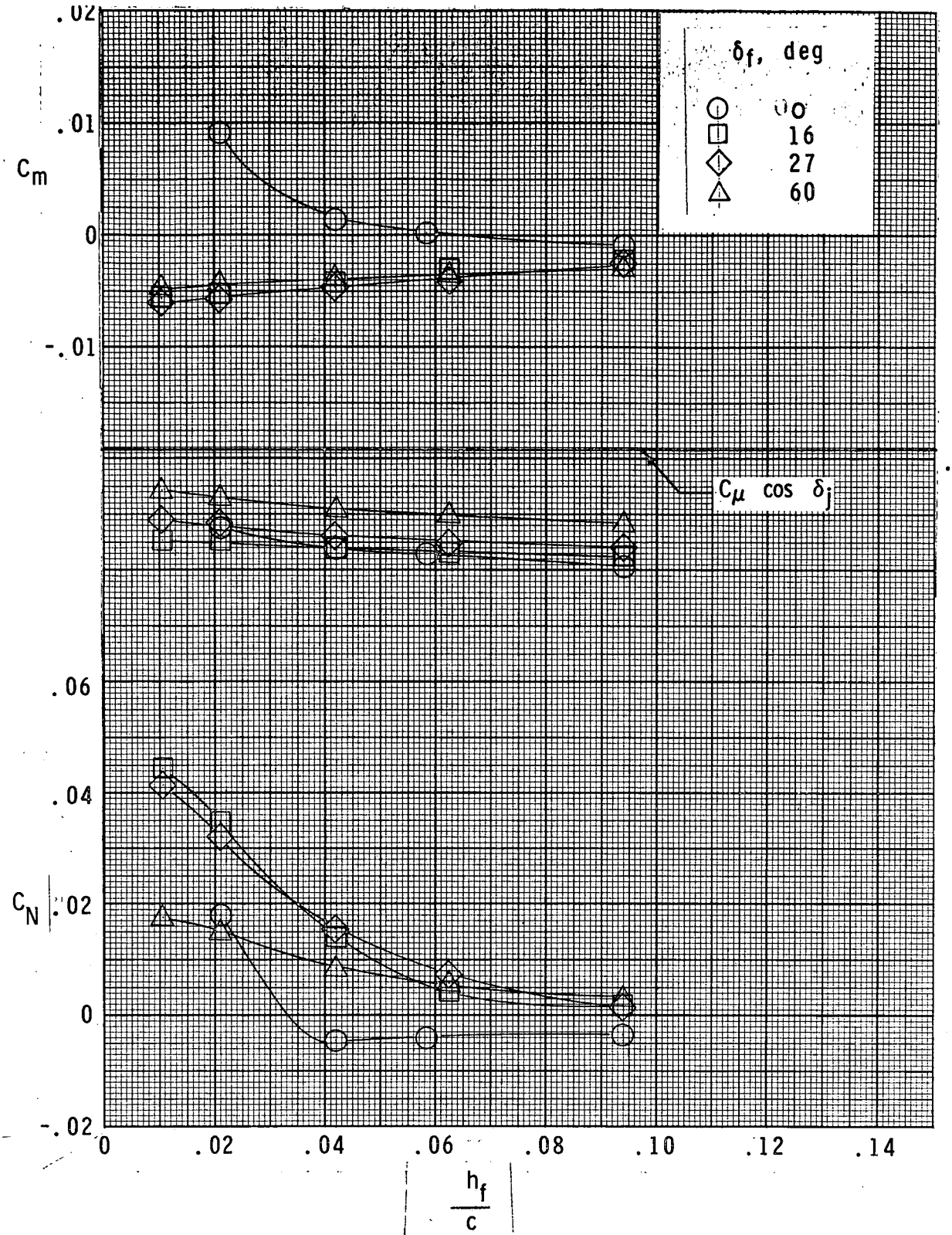

(b) $\alpha = 4^\circ$, $\delta_j = 13^\circ$.

Figure 3.- Continued.

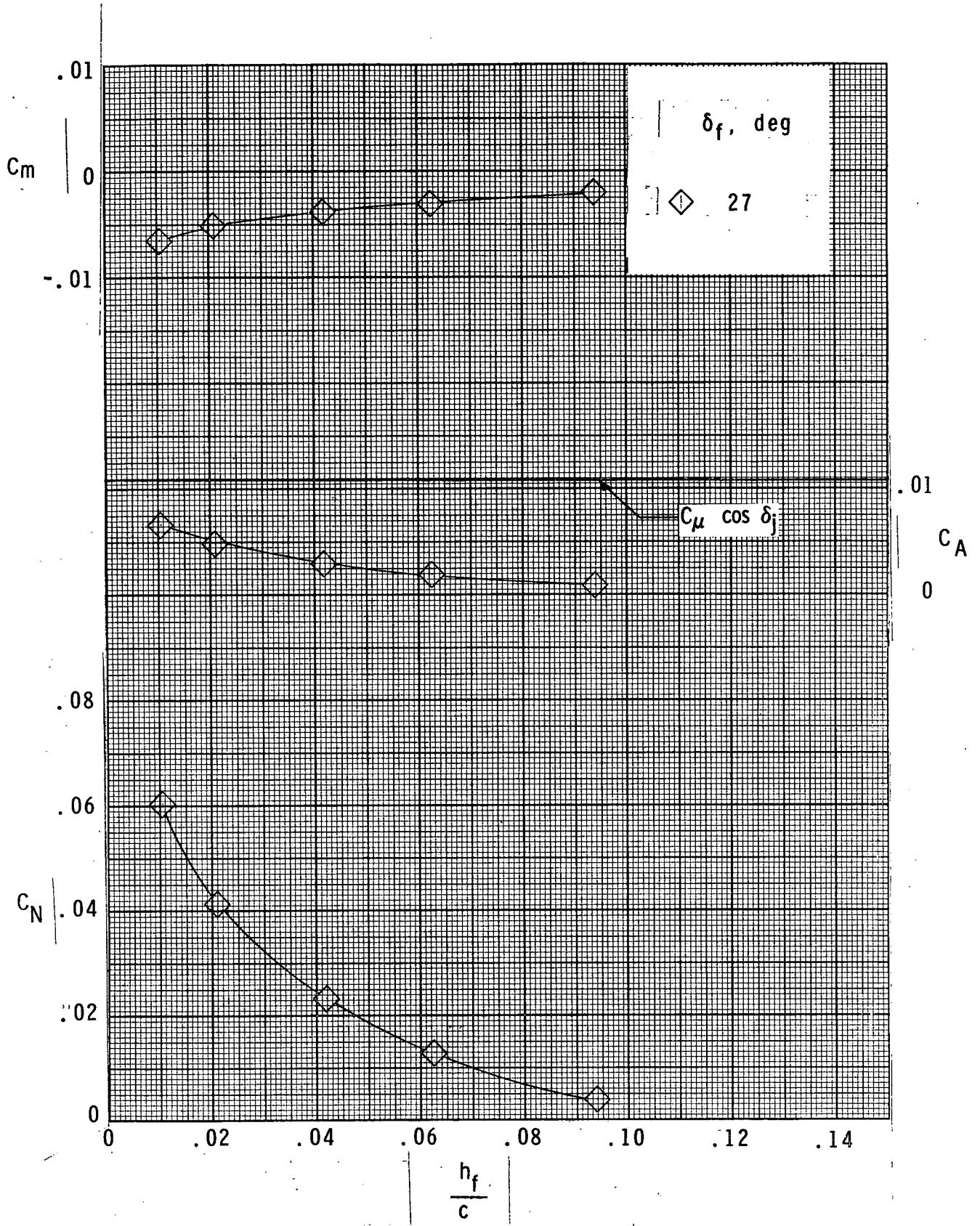

(c) $\alpha = 0°$, $\delta_j = 25°$.

Figure 3.- Continued.

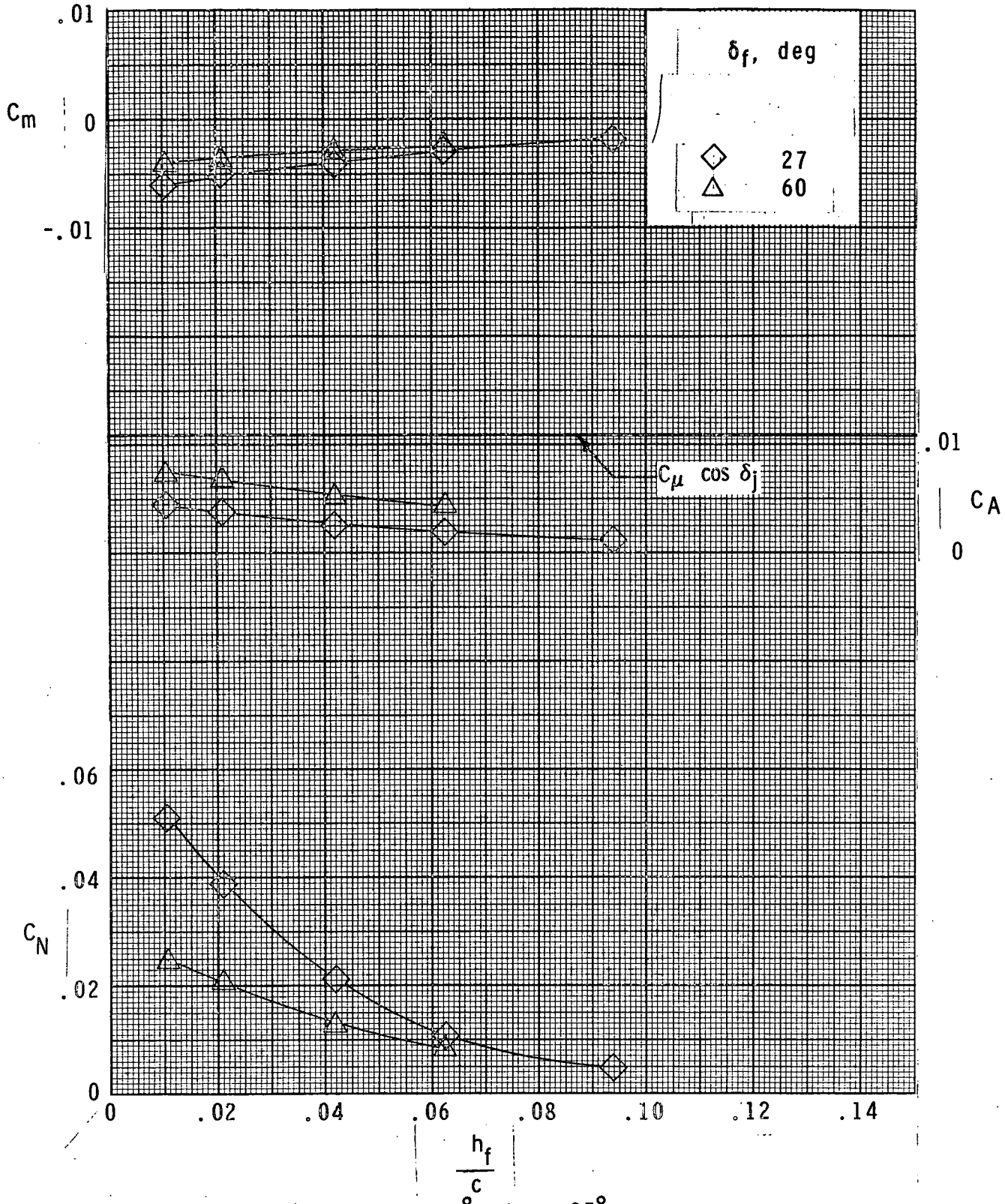

(d) $\alpha = 4^\circ$, $\delta_j = 25^\circ$.

Figure 3.- Concluded.

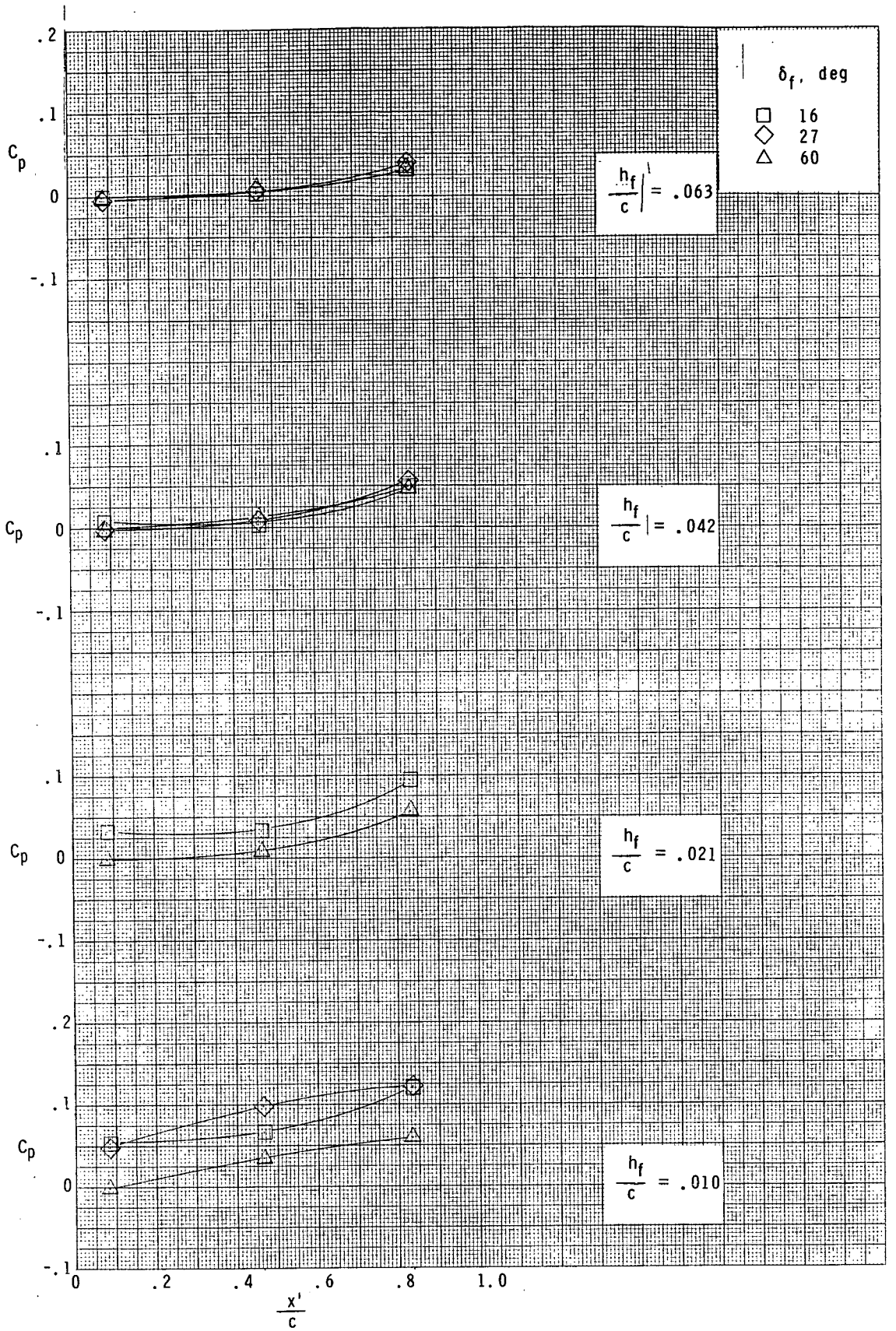

(a) $\alpha = 0°$, $\delta j = 13°$.

Figure 4.- Selected ground-board pressure distributions under the wing and at the jet center line.

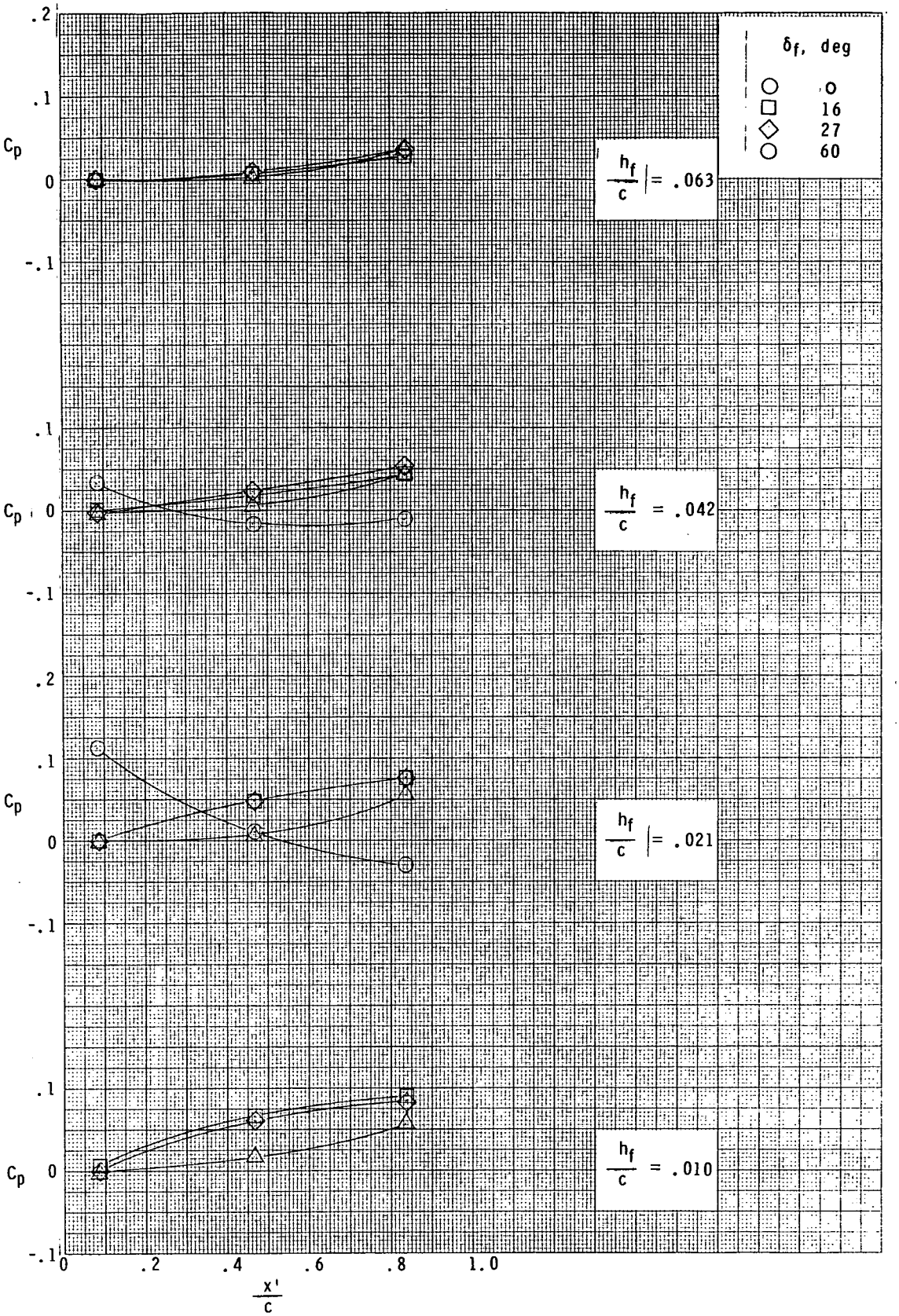

(b) $\alpha = 4°$, $\delta_j = 13°$.

Figure 4.- Continued.

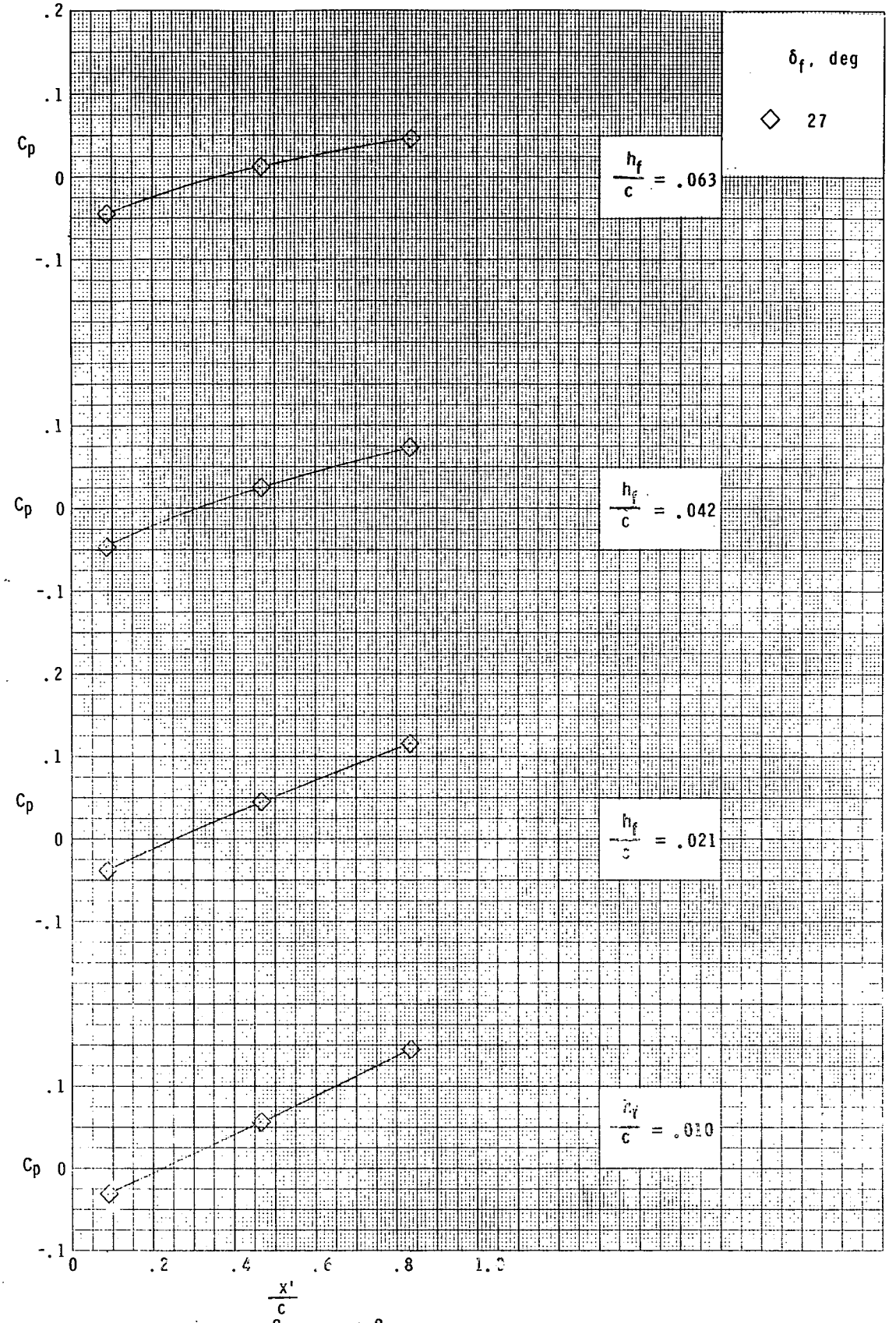

(c) $\alpha = 0°$, $\delta_j = 25°$.

Figure 4.- Continued.

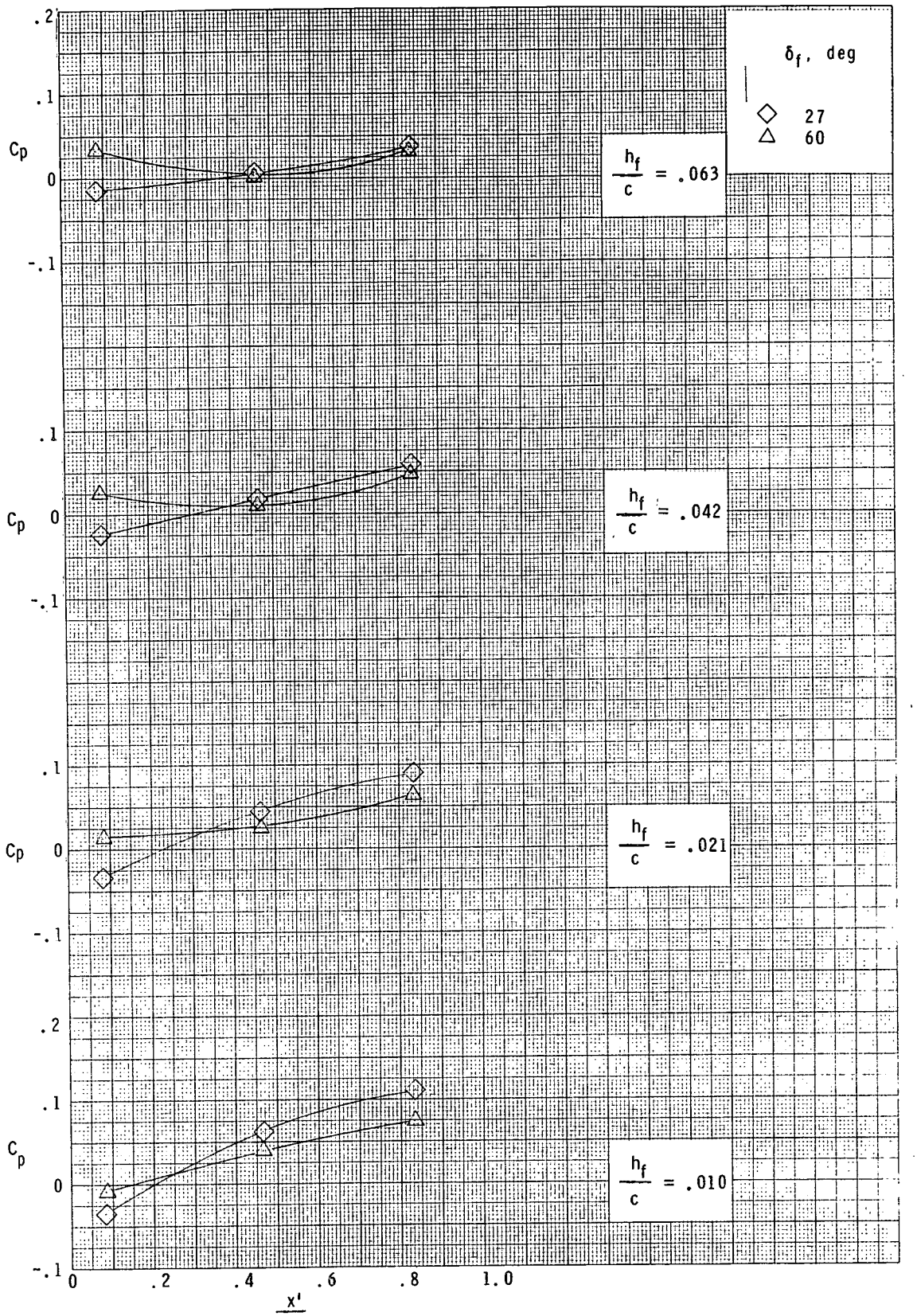

(d) $\alpha = 4°$, $\delta_j = 25°$.

Figure 4.- Concluded.

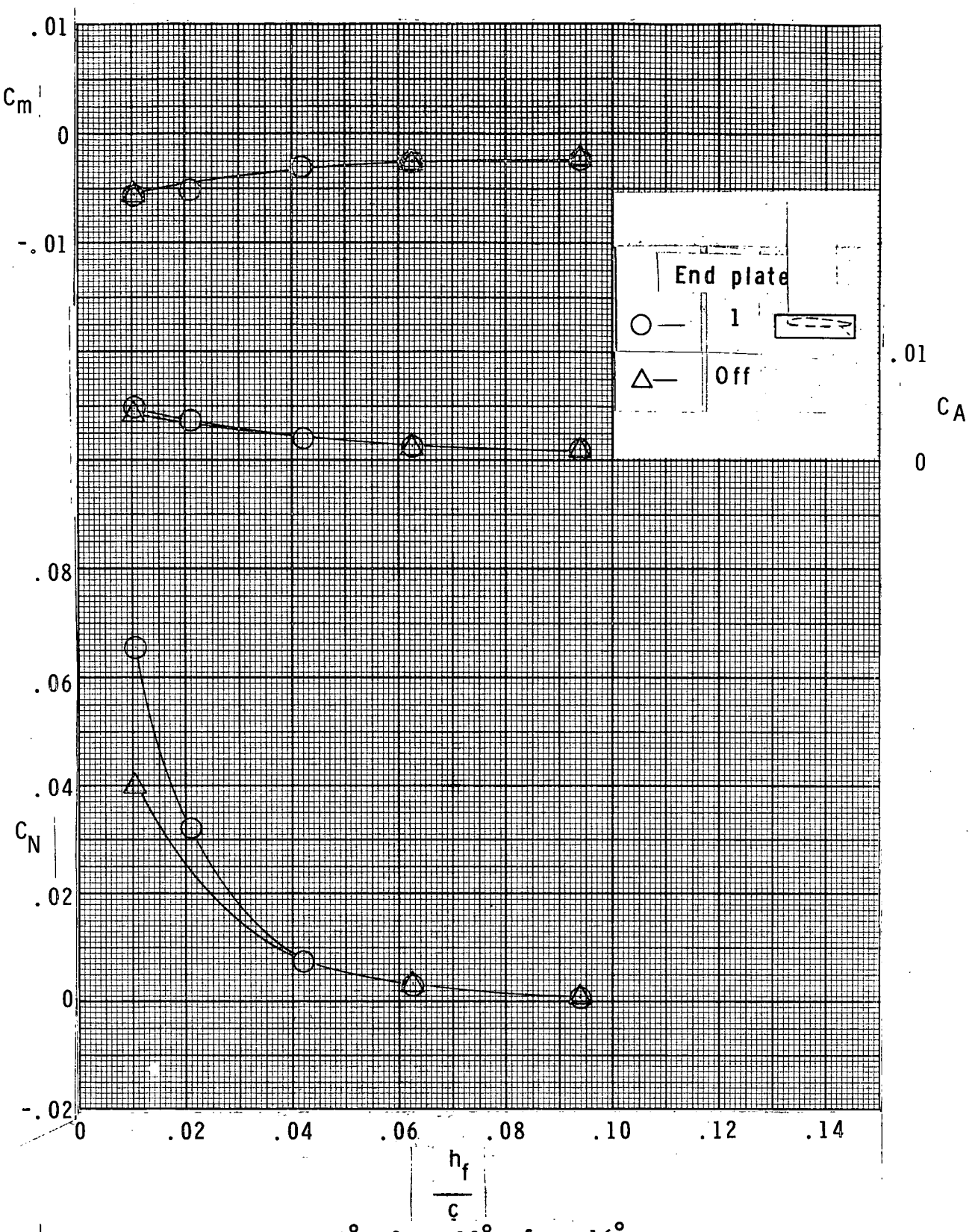

(a) $\alpha = 0^\circ$, $\delta_j = 13^\circ$, $\delta_f = 16^\circ$.

Figure 5.- Effect of end plate geometry on longitudinal aerodynamic characteristics.

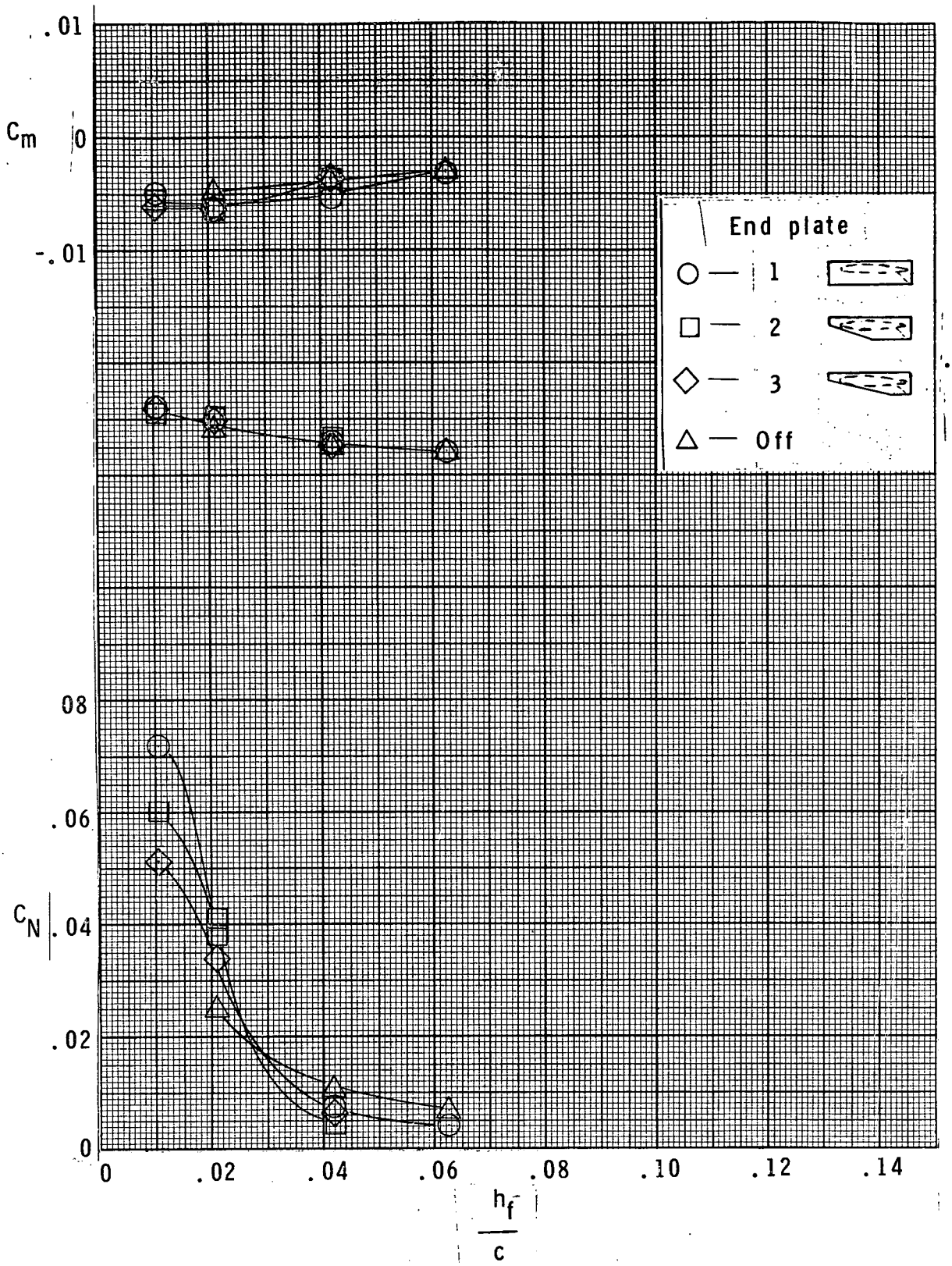

(b) $\alpha = 0°$, $\delta_j = 13°$, $\delta_f, = 27°$.

Figure 5.- Continued.

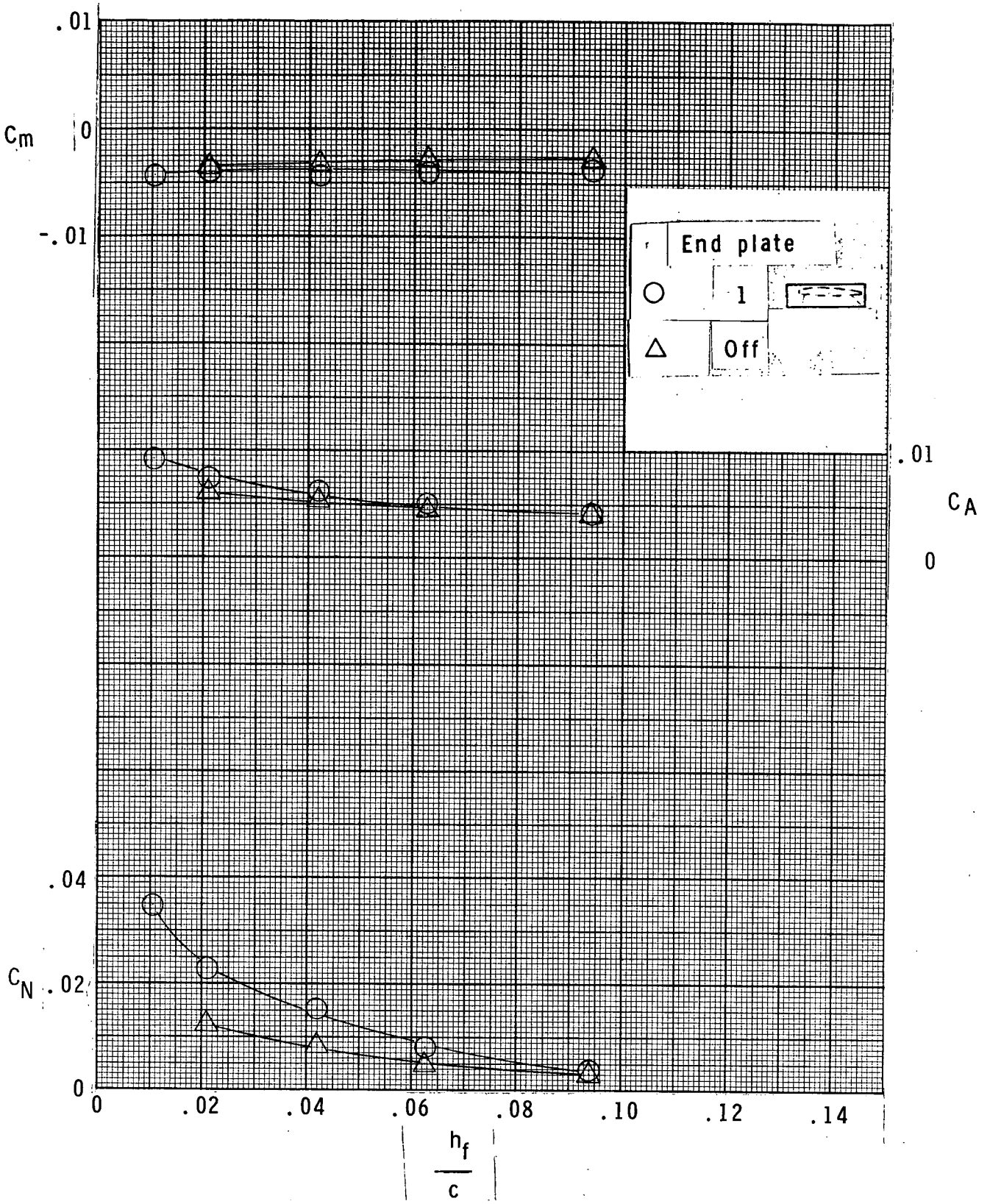

(c) $\alpha = 0^\circ$, $\delta_j = 13^\circ$, $\delta_f = 60^\circ$.

Figure 5. - Continued.

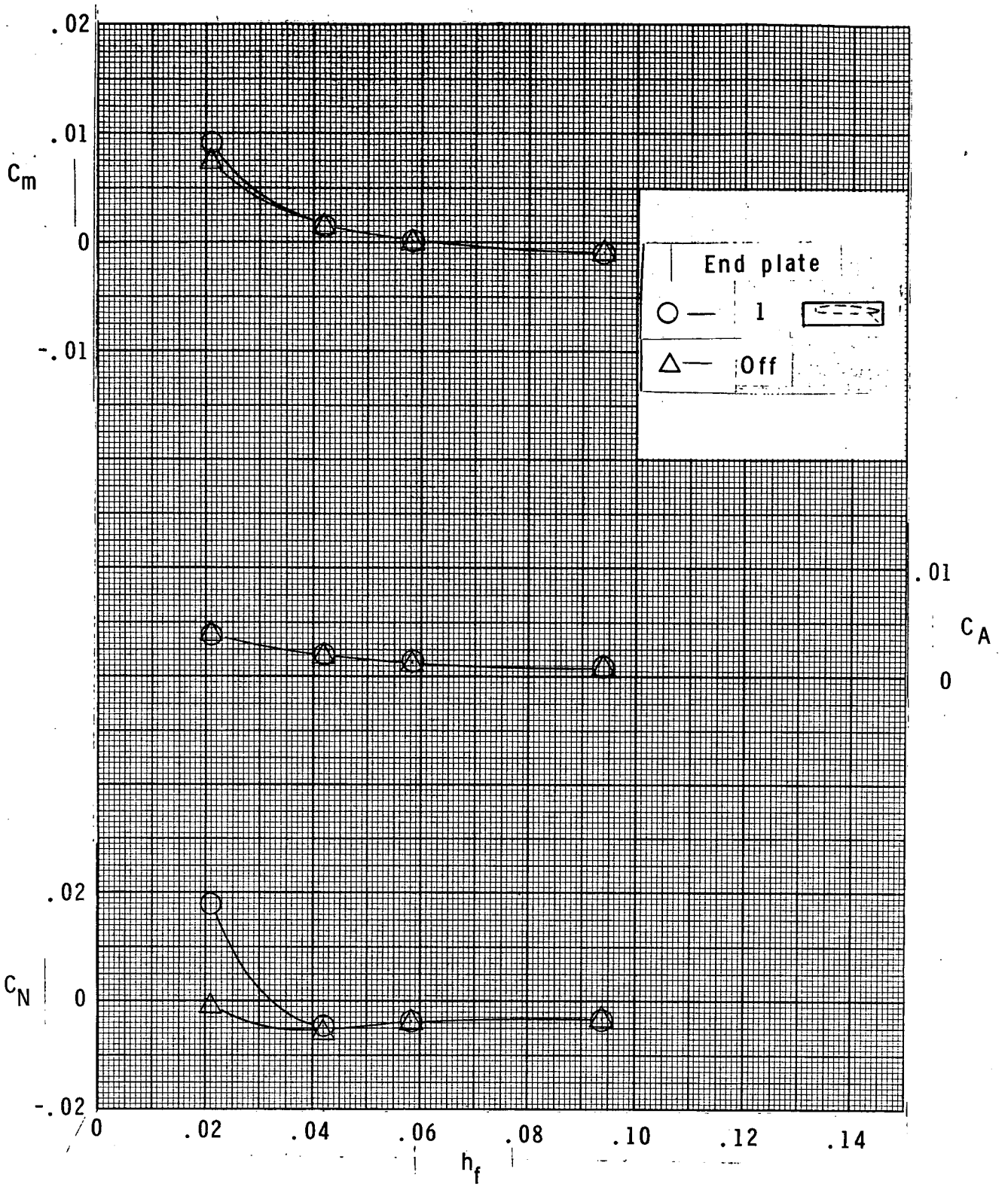

(d) $\alpha = 4^\circ$, $\delta_j = 13^\circ$, Flap off.

Figure 5.- Continued.

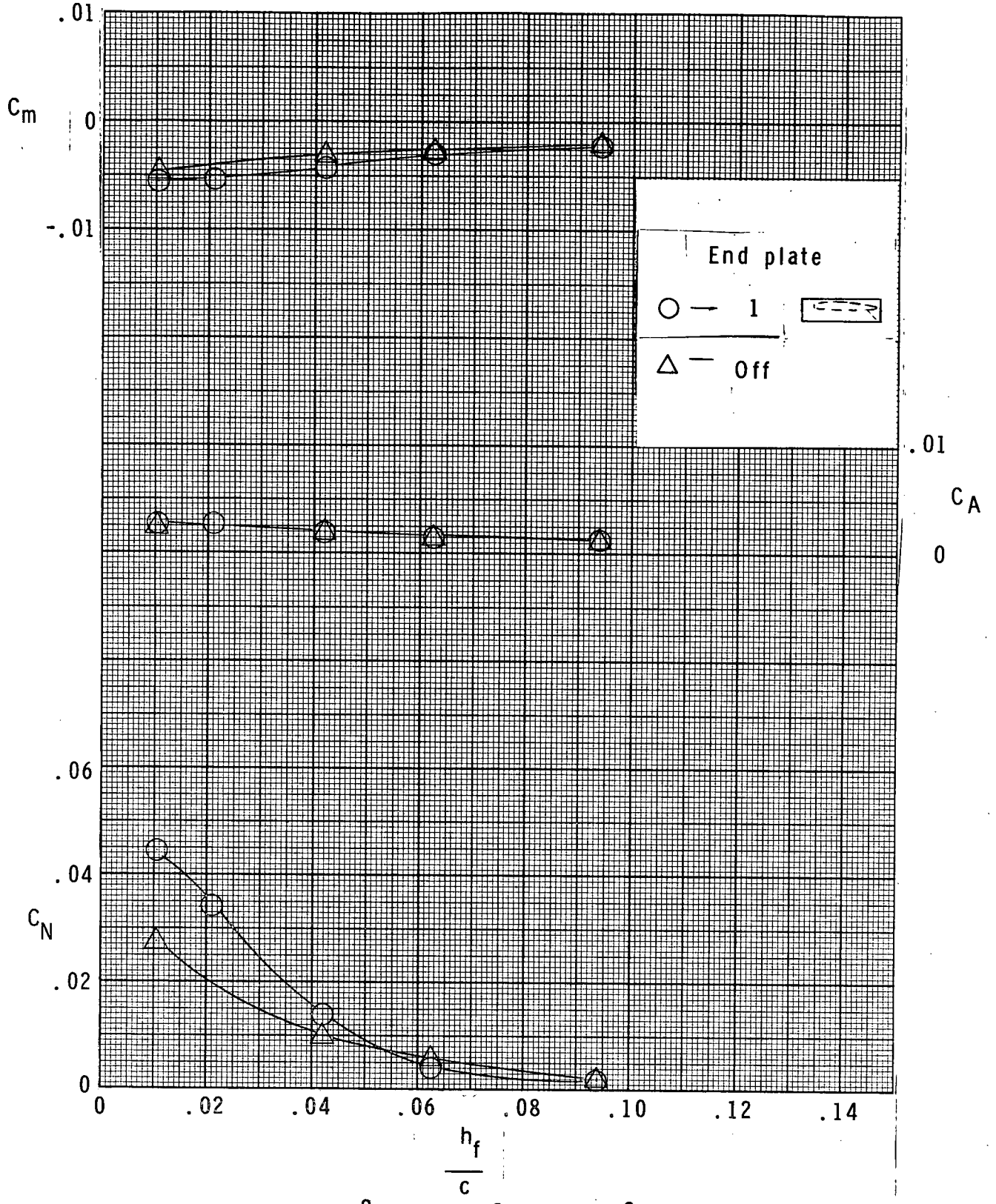

(e) $\alpha = 4^\circ$, $\delta_j = 13^\circ$, $\delta_f = 16^\circ$.

Figure 5. - Continued.

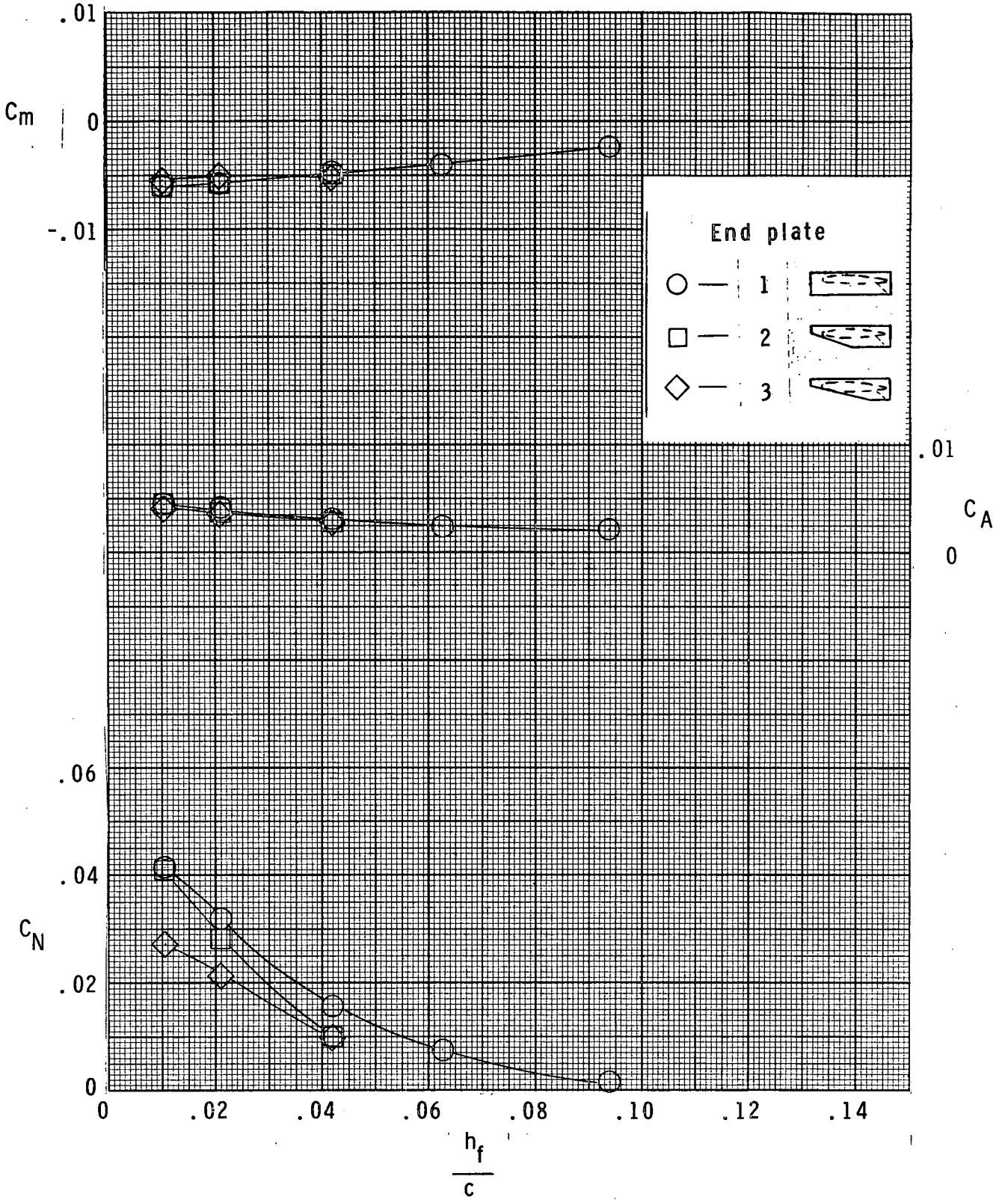

(f) $\alpha = 4^\circ$, $\delta_j = 13^\circ$, $\delta_f = 27^\circ$.

Figure 5. - Continued.

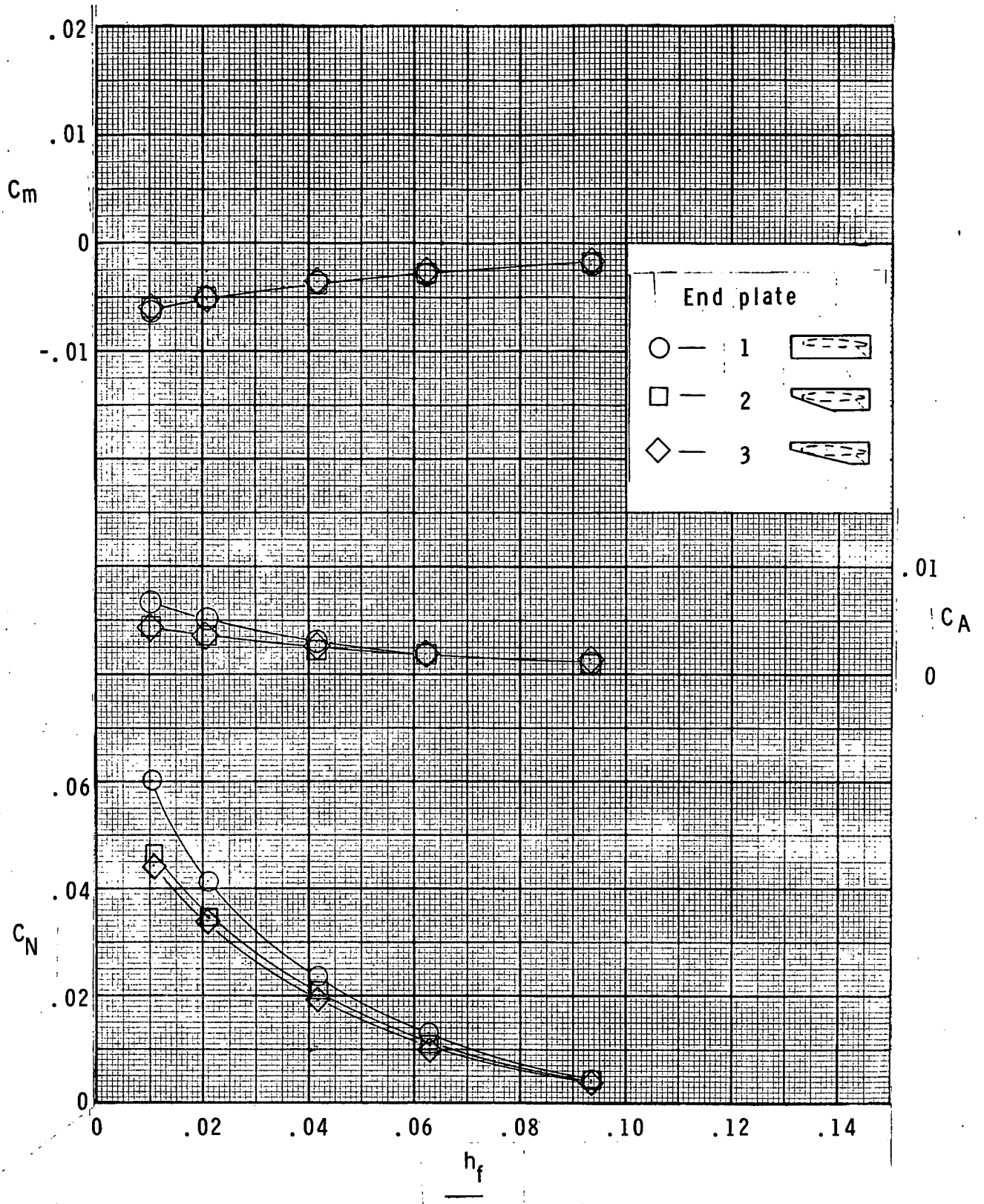

(g) $\alpha = 4°$, $\delta_j = 25°$, $\delta_f = 27°$.

Figure 5. - Continued.

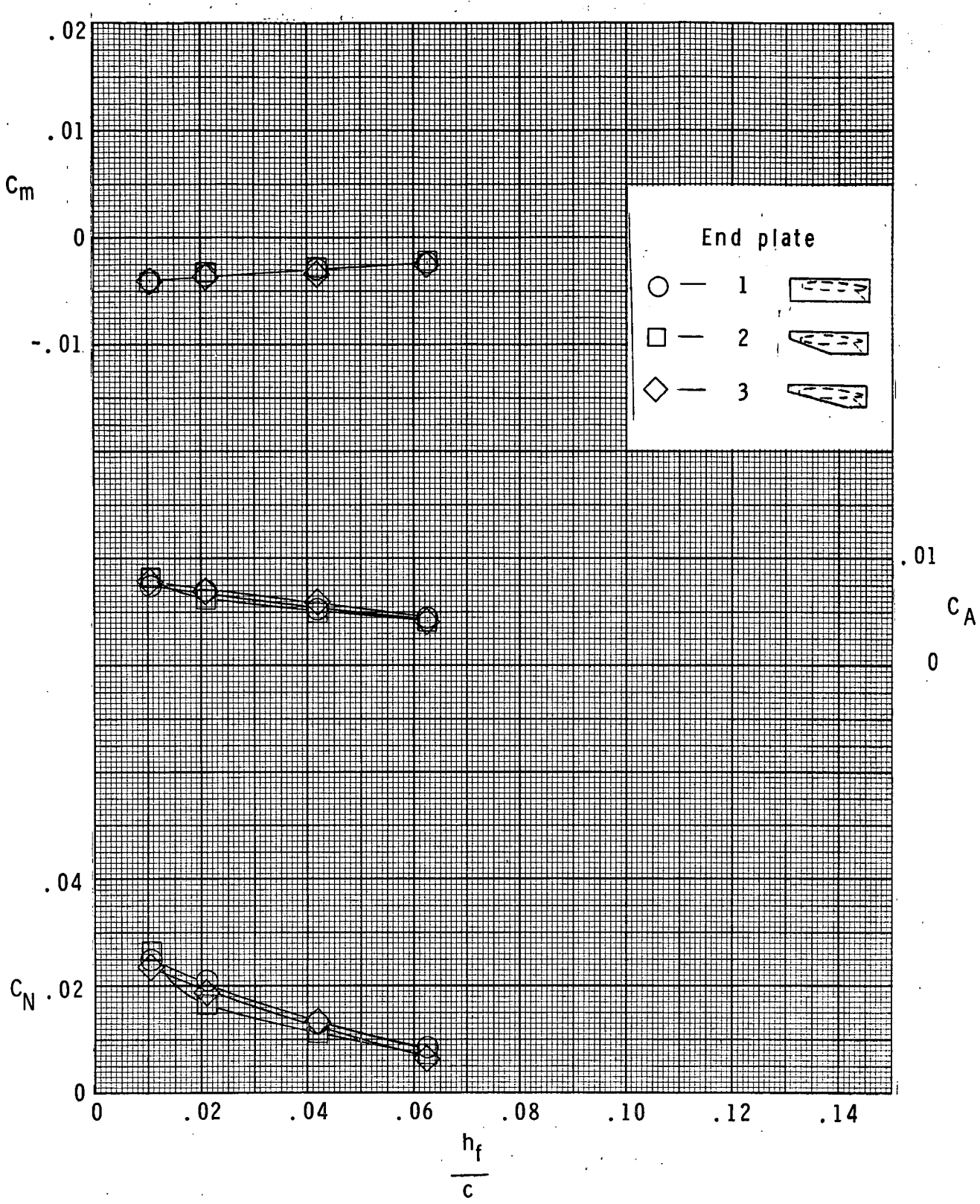

(h) $\alpha = 4^\circ$, $\delta_j = 25^\circ$, $\delta_f = 60^\circ$.

Figure 5.- Concluded.

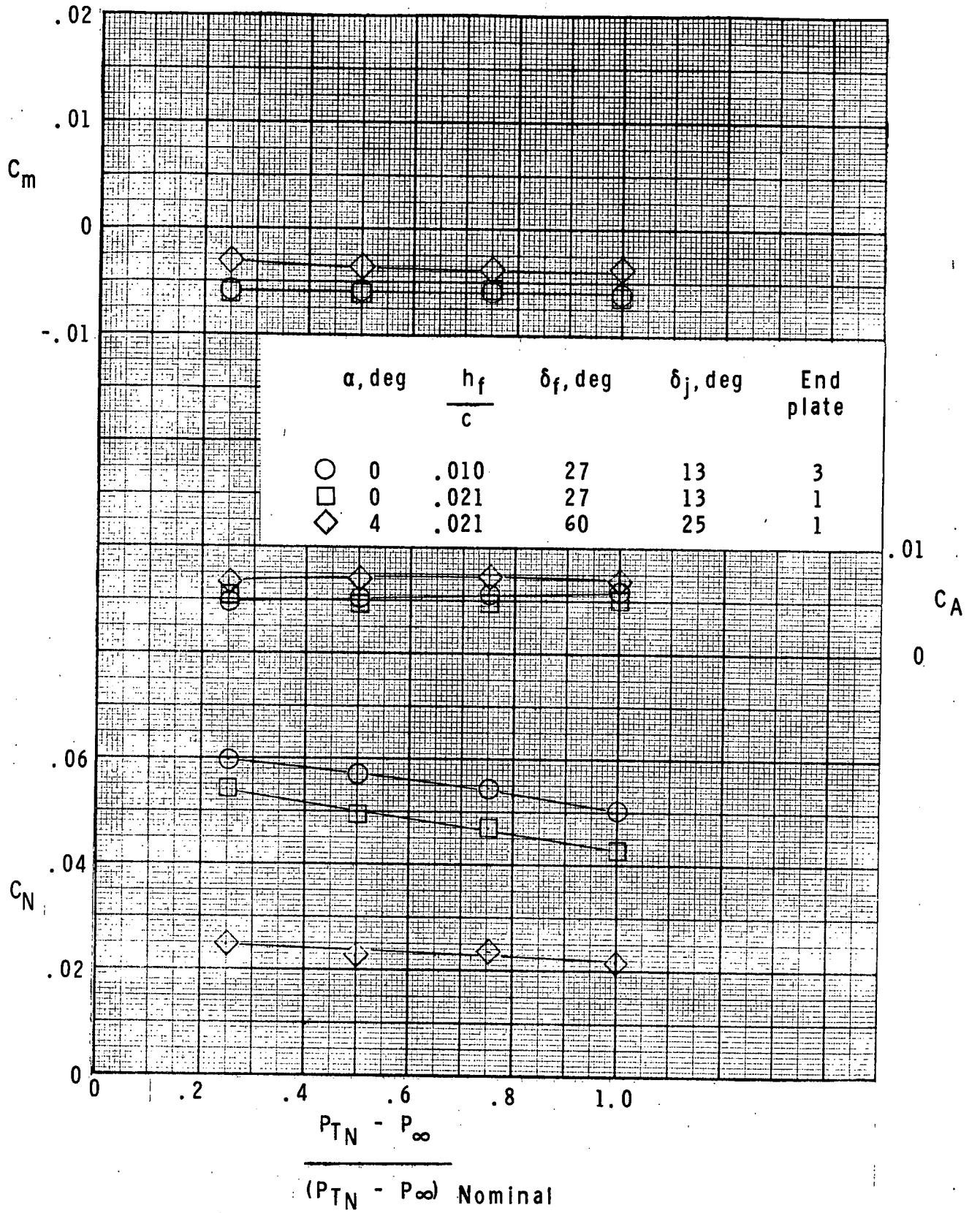

Figure 6.- Effects of reduced jet efflux for selected conditions.

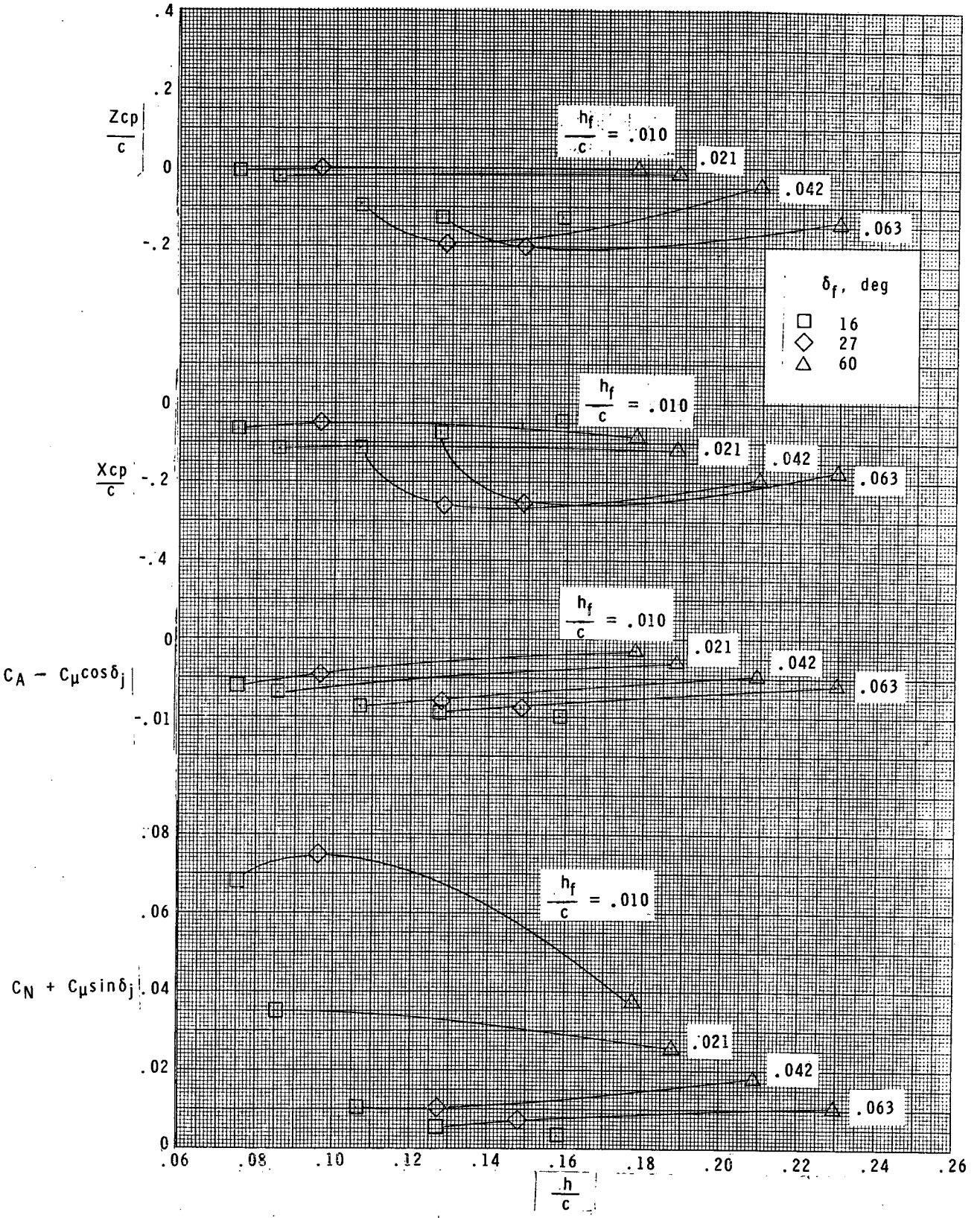

(a) $\alpha = 0°$, $\delta_j = 13°$.

Figure 7.- Summary of net performance of static air cushion system (c_μ = .0109).

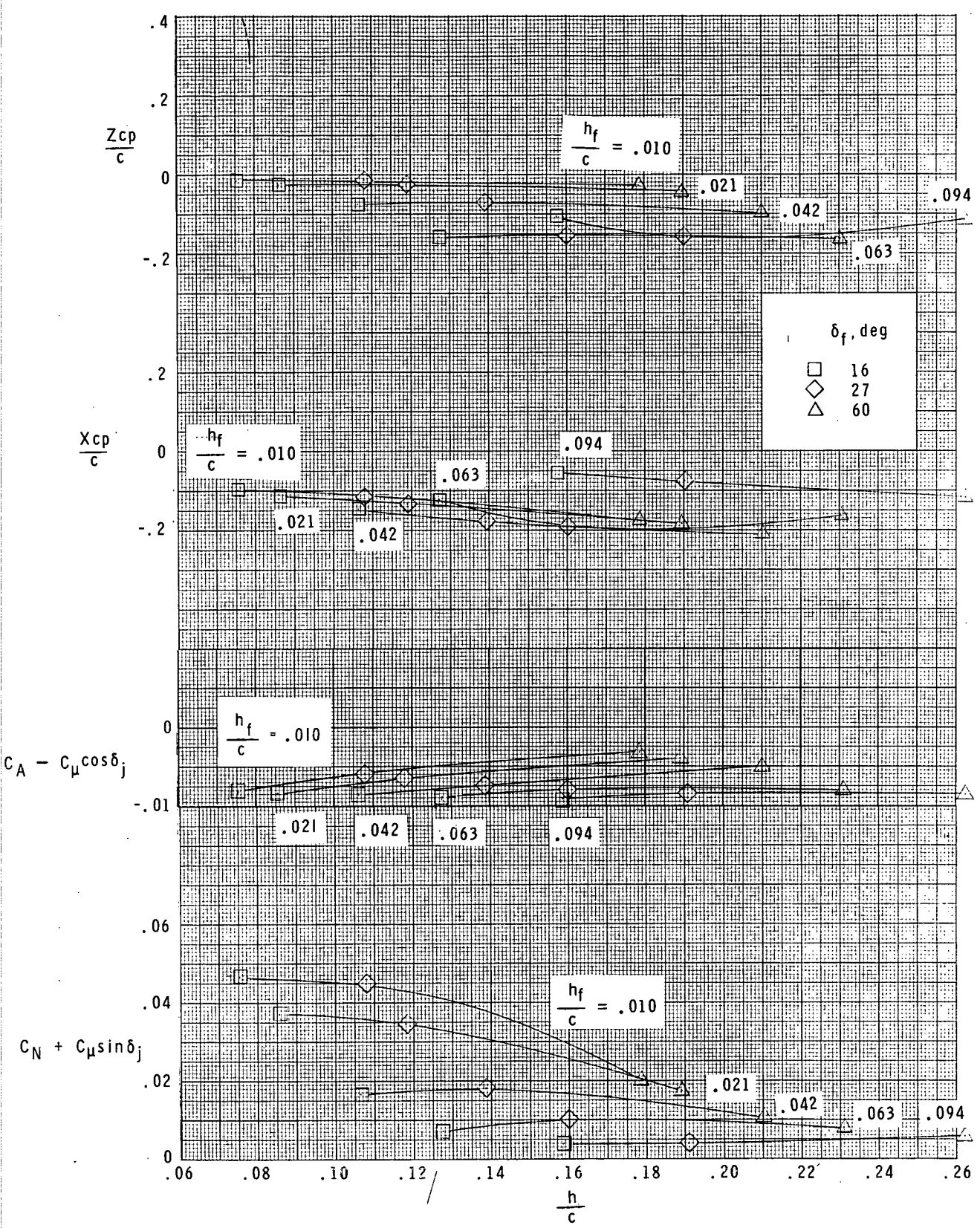

(b) $\alpha = 4°$, $\delta_j = 13°$.

Figure 7.- Continued.

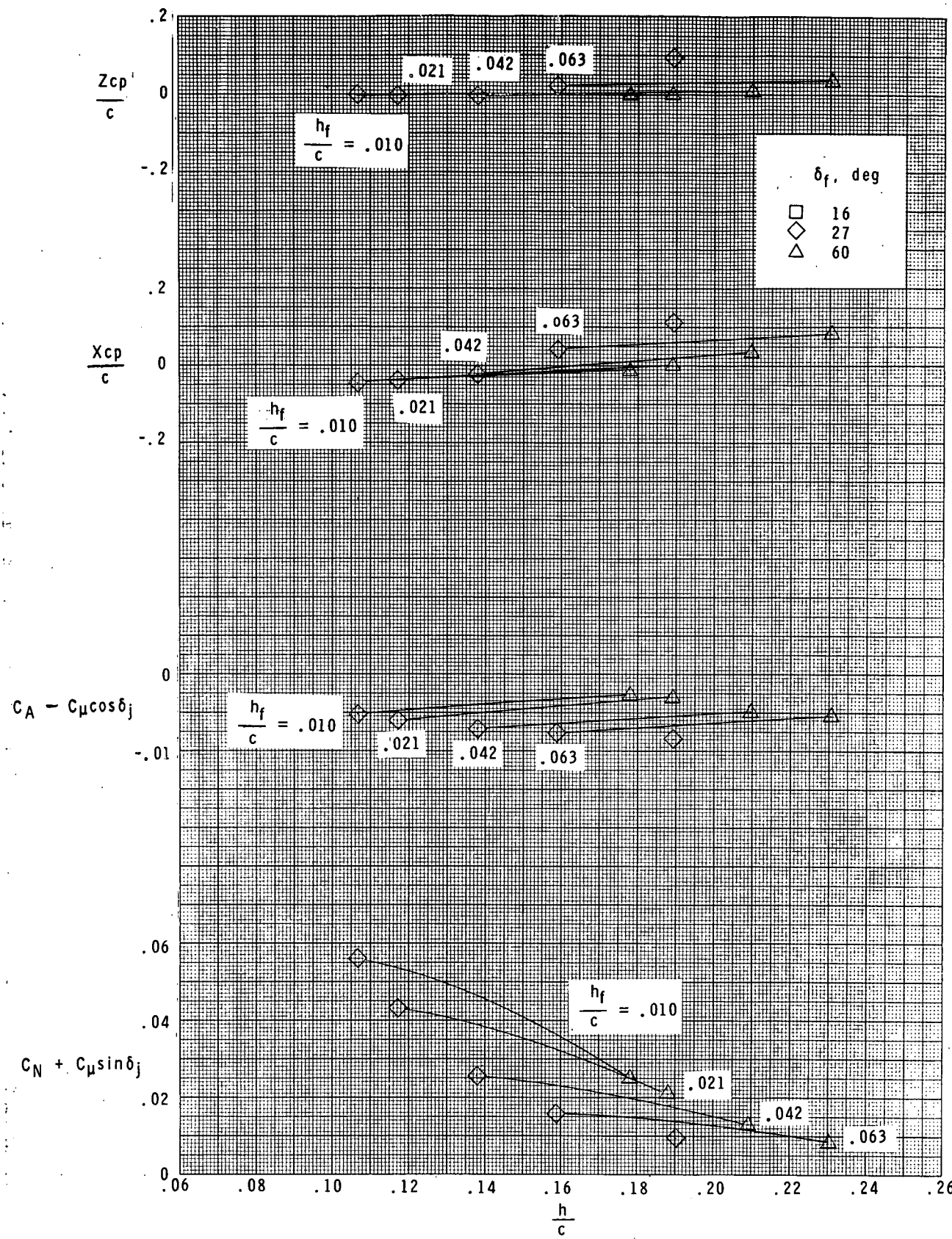

(c) $\alpha = 4°$, $\delta_j = 25°$.

Figure 7.- Concluded.

LWP - 1083

LANGLEY WORKING PAPER

INVESTIGATION OF THE STATIC LIFT CAPABILITY OF A LOW-ASPECT-RATIO WING OPERATING IN A POWERED GROUND-EFFECT MODE

By Jarrett K. Huffman and Charlie M. Jackson, Jr.

Langley Research Center
Hampton, Va.

NATIONAL AERONAUTICS AND SPACE ADMINISTRATION

December 1, 1972